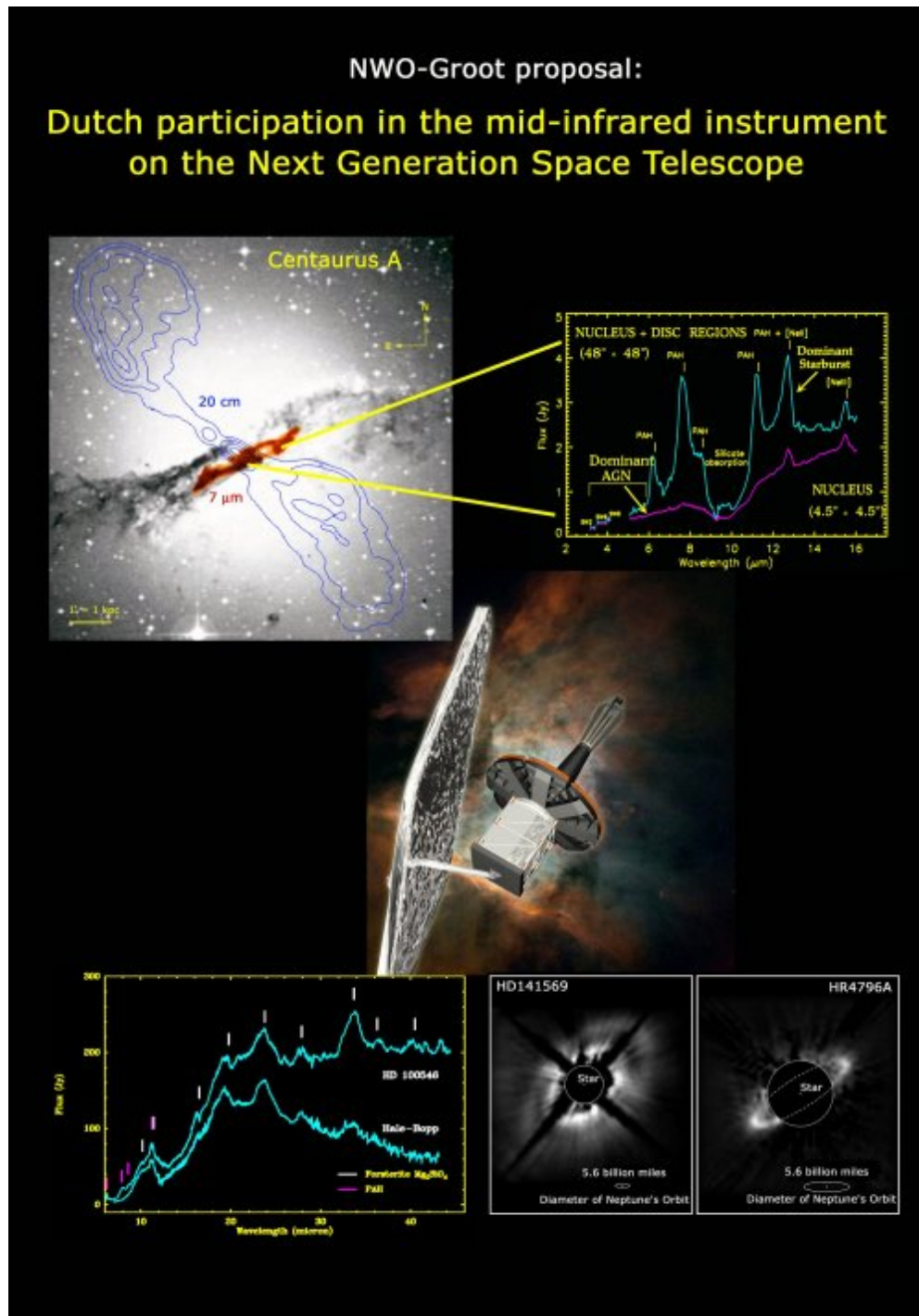


Science Case

MIRI spectrometer for NGST

Extract from www.astron.nl (projects, MIRI/NGST)

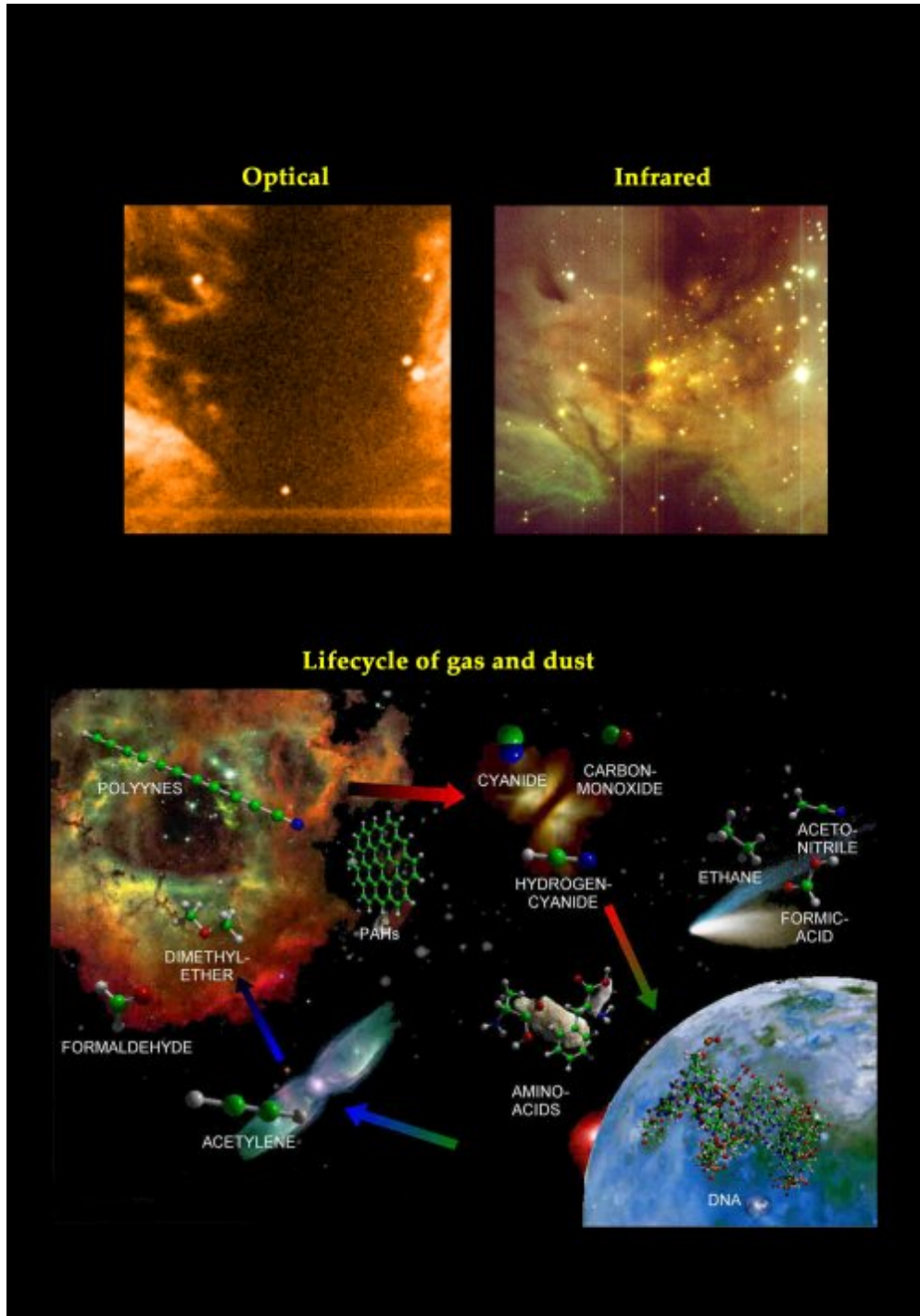
Science Contact: ewine@strw.leidenuniv.nl



Top: Mid-infrared 7 μm image obtained with the camera on the Infrared Space Observatory ISO (orange image in center) and 20 cm radio continuum

contours, superposed on an optical image of the nearest active galaxy Centaurus A. Only the mid-infrared data reveal a warped disk of hot dust near the nucleus. Spectra taken at different positions can distinguish the energy sources responsible for the emission (Mirabel et al 1999).

Bottom: Images of protoplanetary disks taken with the Hubble Space Telescope in near-infrared light, together with the mid-infrared spectrum of one such disk obtained with the ISO-Short Wavelength Spectrometer (Malfait et al. 1998). Note the wealth of mid-infrared features and the similarity with the spectrum of comet Hale-Bopp.



Top: Left: An optical (R-band) image of the field centered on the bright infrared source IRS2, in the Flame Nebula in Orion (North to the top, East to the left, image obtained from the Digital Sky Survey). Apart from the bright emission from ionized hydrogen, virtually no stars are detected. In particular, the center of the field, at the location of IRS2, is totally obscured by surrounding gas and dust. Right: A near-infrared image of the same field, which reveals the central cluster of young massive stars including IRS2, showing that at infrared wavelengths the extinction is much less severe (Lenorzer et al. 2001).

Bottom: The cycle of organic molecules in the universe. The molecules formed in interstellar clouds are transported through circumstellar disks to small solid bodies in new planetary systems such as comets and asteroids. Impacts of these objects may deliver these species on new planets. In the final stages of stars, dust and elements are returned to the interstellar medium (figure by R. Ruitkamp, based on Ehrenfreund & Charnley 2000).

Table 1. Overview of the NGST mission

Mission type:		General purpose astronomical observatory
Telescope:	Type	Three mirror anastigmat
	Primary	6.5 meter segmented mirror
	Image quality	Diffraction limited at 2 μm (0.08")
Spacecraft:	Orbit	Sun-Earth Lagrange 2 halo orbit
	Mission lifetime	5 years – consumables for 10 years
Payload:	Wavelengths	0.6–28 μm
	Thermal	Passively cooled to 50 K
	Stray light	Sky-dominated below 10 μm
	Sky coverage	Instantaneous: >15%; Yearly: whole sky
Instrument modules:	Type	Near-infrared camera 0.6–5 μm
		Near-infrared multi-object spectrometer 1–5 μm , R~1000
		Mid-infrared camera/spectrometer 5–28 μm , R~3000 goal
	Total mass	<1000 kg
Expected launch date:		2009

The key aim will be to chart the history of star formation in the universe all the way from the present, where the star- and planet formation process can be studied in detail, to the dawn of time when the first stars formed and galaxies were assembled. A large space telescope at infrared wavelengths is the logical choice for these programs, since for the most distant galaxies, lines such as H Lyman-alpha at 1216 Å are shifted to the red part of the spectrum, where the ground-based sky brightness is high and the objects themselves are becoming very faint. This history of star formation is of course intimately interwoven with the origin of the elements in the universe because as stars evolve they enrich their environment with freshly synthesized elements which then become available for the next generation of stars. Star formation is also closely linked to the formation of planetary systems – which are now known to be widespread – and the origin of life thereon.

Much progress in these areas will have to come from the mid-infrared part of the spectrum as the formation of stars and planets occurs in the deeply enshrouded environment of molecular clouds and disks, hidden from visible view by copious amounts of small dust grains. The observations at long wavelengths allow astronomers not only to lift this obscuring veil (see back-cover), but also to study the dust itself. Indeed, the mid-infrared wavelength range is particularly rich in diagnostic spectroscopic features and it is the only region where the dominant molecule H₂ – the principal ingredient of gaseous giant planets – and the solid state species can be studied directly.

The mid-infrared instrument on NGST is expected to revolutionize our understanding of these problems since it will have unprecedented sensitivity and spatial resolution. [Figure 1](#) illustrates the expected imaging and spectral sensitivity compared with other facilities. NGST will be three orders of magnitude more sensitive than any ground-based telescope in the 5–30 μm range, a large part of which (>50%) is completely inaccessible from the ground due to absorption by the Earth's atmosphere. Moreover, even within the atmospheric windows, ground-based observations are limited by atmospheric conditions to less than 50% of the night time, even at good mid-infrared sites. Compared with SIRTf (the 85-cm NASA Space Infrared Telescope Facility, to be launched in 2002), NGST will have more than an order of magnitude increase in sensitivity and spatial resolution. Moreover, SIRTf will have only very low resolution spectroscopy $R = \lambda/\Delta\lambda = 50\text{--}100$ in the important 5–10 μm range, and only $R = 600$ in the 10–38 μm range. Such low resolving powers are insufficient for many key scientific programs ([section II.1](#)). Thus, NGST has the potential to perform unique science in a poorly explored wavelength range, increasing substantially the discovery space.

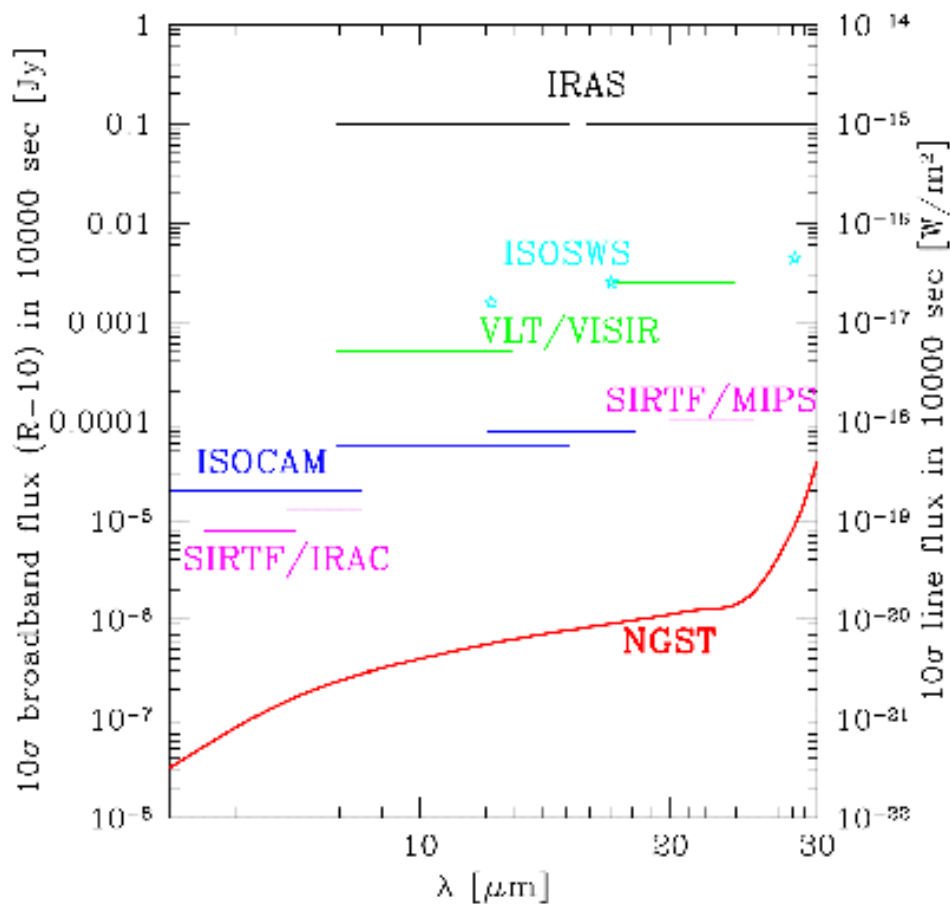


Figure 1. Imaging (left scale) and spectral (right scale) sensitivity of NGST (orange line) compared with previous space missions (IRAS, ISO), future space missions (SIRTIF) and future ground-based instruments (VISIR on the 8m ESO-VLT). The ISO-SWS stars (light-blue) refer to the flux scale, all other facilities refer to the broad-band flux scale.

The mid-infrared instrument will be built jointly by NASA and ESA in a 50%–50% partnership. The European consortium will be led by the UK and includes at least France, Germany and Italy. At the NGST Mid-Infrared Steering Committee (MISC) meeting in July 2001 in the UK, the basic instrument characteristics (Table 2) and division of labor were agreed between the US and Europe. Here we request funding for the Netherlands to make a critical contribution to the European consortium which will ensure that the spectrometer part of the instrument is built with the desired spectral resolution and integral field capability. The initial 7-month instrument design study (phase A) will be partly financed by ESA and the applicants, and will start in Fall 2001. The subsequent Phase B/CD design and construction will start in the spring of 2003, with instrument delivery planned for 2007/2008.

Table 2. Top-level specifications of the NGST mid-infrared instrument

Mode	Requirements
Imaging	Wavelength range 5–27 μm
	Diffraction limited imaging, Nyquist sampled at no longer than 8 μm
	Minimum field of view of 1.5 arcmin
	Filter wheel with at least 8 spectral bands: 4–5 for SED definition,

remainder for PAH isolation, brown dwarf atmosphere color
identification

Simple coronagraph

Larger imaging field of view a goal

Spectroscopy Single object, 5–27 μm , important goal to extend to 28.3 μm
Resolution R ~ 100 from 5–10 μm
Resolution R ~ 1000 –3000 from 5–28.3 μm
Resolution close to 3000 (or slightly higher) to be a goal

II. Science case

The scientific case for the mid-infrared instrument on NGST has been described previously by Serabyn et al. (1999), Wright et al. (1999) and van Dishoeck (2000). The general NGST science program is contained in the *Design Reference Mission*, a set of strawman observing proposals written by the NGST Ad Hoc Science Working Group (ASWG) (see [Appendix G](#)). It was most recently summarized in the NGST proposal to ESA in July 2000 (ESA-SCI(2000)9). This proposal led to the confirmation of the ESA participation in NGST in October 2000. Dutch astronomers have actively participated in defining these science cases.

In the following, a brief overview of the rich variety of features at mid-infrared wavelengths will be given, followed by a selection of scientific topics which highlight the spectroscopic applications of interest to the NOVA research program. One of the main benefits of a Dutch investment in the mid-infrared instrument is that it will allow Dutch astronomers to be part of the mid-infrared science team that defines the observing programs for the guaranteed time. As always with new instruments, the most exciting science will likely come from unexpected discoveries in areas which have not even been considered. The enormous increase in sensitivity and spatial resolution with NGST will virtually guarantee such serendipitous results.

II.1. Mid-infrared features

In the local universe, the continuum at mid-infrared wavelengths is dominated by thermal emission from warm dust with $T_{\text{dust}} \sim 100$ –300 K, such as found in star-forming regions and around late-type stars (red giants, so-called Asymptotic Giant Branch (AGB) stars). The ultraviolet and optical radiation from these stars is absorbed by the dust and re-radiated at longer wavelengths. In addition, thermal emission from the atmospheres of cool stars, from brown dwarfs with effective temperatures $T_{\text{eff}} \sim 1000$ K, and from solar-system objects such as comets and Kuiper-Belt objects is significant at mid-infrared wavelengths. Any non-thermal (synchrotron) contribution is generally small.

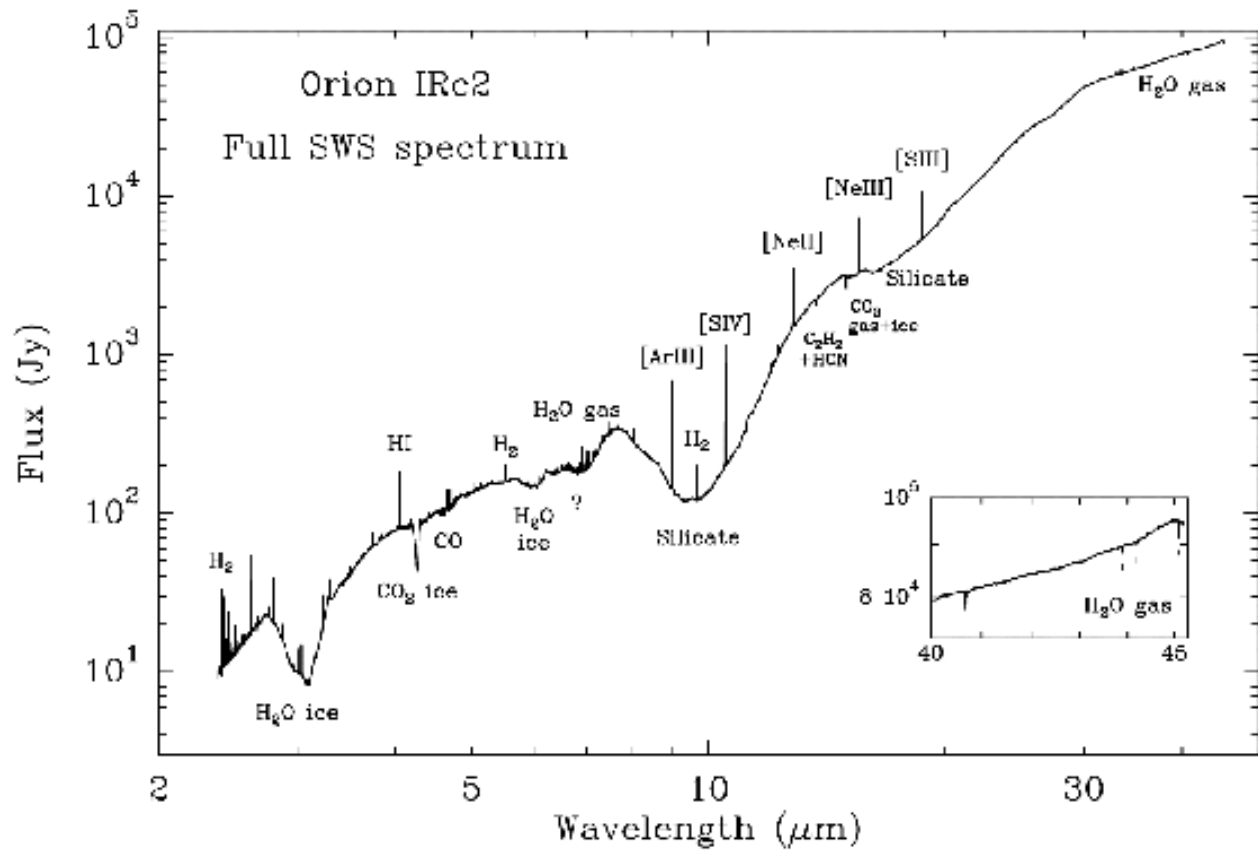


Figure 2. Complete ISO-SWS grating spectrum centered at Orion IRC2 at a resolving power $R=1300\text{--}2500$. The principal absorption and emission features are indicated. The ISO-SWS beam ranges from $14'' \times 20''$ to $20'' \times 27''$, and encompasses both the IRC2 and BN sources (van Dishoeck et al. 1998).

The mid-infrared is rich in spectral features, many of which are unique for this wavelength range. They are illustrated in the ISO Short Wavelength Spectrometer (SWS) spectrum of one of the brightest mid-infrared sources in the sky, the Orion-KL region (Figure 2) and are summarized in Table 3. Each of the categories of features is discussed below, together with their diagnostic value.

Table 3. Some important spectral features in the mid-infrared

Category	Wavelength (μm)	Species	Diagnostic ^a
Ions	7.0	[Ar II]	Radiation field
	9.0	[Ar III]	Shocks
	10.5	[S IV]	Spectral index
	12.8	[Ne II]	Density
	14.3	[Ne V]	Metallicity
	15.6	[Ne III]	
	18.7	[S III]	

	25.2	[S I]	
	25.9	[O IV]	
PAHs	6.2, 7.7, 8.6, 1.3 12.7, 14.2, 16.2		Carbonaceous material, UV, Redshift obscured galaxies
Silicates (Amorphous)	9.7 18.0		Bulk of dust
Silicates (Crystalline)	10.0, 11.3, 16.3, 19.5 23.5, 27.5	Mg ₂ SiO ₄	Mineralogy, Heating events Solar system connection
	18.5, 21.5, 24.5	(Mg,Fe)SiO ₃	(meteorites, IDP's, ...)
Oxides	11.6	Al ₂ O ₃	
	23	FeO	
Sulfides	23	FeS	Gas-solid chemistry
Carbonates	6.8, 11.3	XCO ₃	Aqueous alteration, formation large bodies
Ices	6.0	H ₂ O	Volatile solid material
	6.8, 9.7	CH ₃ OH	Building blocks complex organics
	7.7	CH ₄	Solar system connection (comets, KBOs)
	9.7	NH ₃	Thermal history
	15.2	CO ₂	
H ₂	6.9, 8.0, 9.7, 12.2, 17.0, 28.2		Mass + temperature of bulk of warm gas Photon- vs shock-heating
HD	19.4, 23.0, 28.5		[D]/[H]
Gas-phase	6.0	H ₂ O	Temperature + density structure
Molecules	7.7	CH ₄	Building blocks complex organics
	13.7	C ₂ H ₂	
	14.0	HCN	
	15.0	CO ₂	

^a Diagnostic properties of category of species; individual species or lines probe a subset of these properties.

Atomic and ionic fine-structure lines: Fine-structure transitions within the lowest electronic term of most astrophysically relevant atoms and ions occur in the 5–30 μm range. Important examples are the [Ar II] 7.0, [Ne II] 12.8, [Ne V] 14.3, [Ne III] 15.6, [S I] 25.2, and [O IV] 25.9 μm lines, but even higher ionization stages ("coronal" lines) can be observed. These features are used as probes of the ionizing source, especially the hardness of the radiation field (e.g., starbursts vs. active nuclei), and as diagnostics of heating mechanisms, in particular shock- vs. photon-heating. The strongest lines can also be used to trace the kinematics of gas in obscured regions.

PAHs: The C–C and C–H stretching and bending modes of polycyclic aromatic hydrocarbons (PAHs) at 6.2, 7.7, 8.6, 11.3, ... μm often dominate the mid-infrared emission. More recently, new features at longer wavelengths have been found in ISO-SWS spectra, which contain important diagnostic information about the mix of species involved (Tielens et al. 2000). Significant variations of factors of five or more can occur in the ratios of various bands (e.g. 8.6/7.7 and 11.3/7.7 μm), which appear related to differences in the ionization and hydrogenation state of the carriers. PAHs contain a significant fraction of the carbon budget and play a role in the energy balance in the interstellar medium. They are also the best redshift indicators for distant, obscured galaxies.

H₂ and HD pure rotational lines: The lowest transitions of the most abundant molecule in the universe, H₂, occur at mid-infrared wavelengths (see [Figure 3](#)). The fundamental $J = 2-0$ S(0) quadrupole line of para-H₂ occurs at 28.22 μm , whereas the next transition, the $J = 3-1$ S(1) line of ortho-H₂, lies at 17.03 μm . Since the populations of these levels are thermalized under many conditions, the S(0) and S(1) lines provide a direct measure of the mass and temperature of the *bulk* of warm molecular gas at $T = 50-200$ K. In contrast, the higher pure rotational lines, as well as the vibration-rotation lines at 2 μm , probe only the small fraction (<1%) of photon- or shock-heated gas in the beam (Draine & Bertoldi 1999, Wright 2000). The heavier isotope, HD, has a small dipole moment and its lowest $J = 1-0$ line at 112 μm has been detected with the ISO-LWS (Wright et al. 1999). The higher $J = 4-3$, $5-4$ and $6-5$ lines occur at 28.5, 23.0 and 19.4 μm . The latter line was observed by Bertoldi et al. (1999) in the Orion shock and can, in combination with H₂ data, be used to determine the [D]/[H] ratio in star-forming regions, providing constraints on the deuterium destruction in stars since its production in the Big Bang.

Solid-state vibrational bands: The characteristic vibrational bands of ices, silicates and oxides occur uniquely at mid-infrared wavelengths. Solid-state species can be distinguished from gas-phase molecules because their bands lack the characteristic ro-vibrational structure and are broadened (see [Figure 4](#)). The presence of H₂O and CO ice mantles surrounding grain cores was established from ground-based observations, but only ISO revealed the complete interstellar ice content and the rich spectral detail. Similarly, the Si–O stretching and bending bands of amorphous silicates at 9.7 and 18 μm were well known, but features of crystalline silicates and oxides at longer wavelengths were discovered only recently by ISO in circumstellar matter around young and old stars (Waters et al. 1996, Waelkens et al. 1996). This wealth of mid-infrared solid-state features was one of the big surprises and legacies of the ISO-SWS. Complete wavelength coverage of the mid-infrared wavelength range allows the full inventory of ices and silicates to be made, whereas their bandshapes and abundances are sensitive diagnostics of heating events and the temperature history of the region.

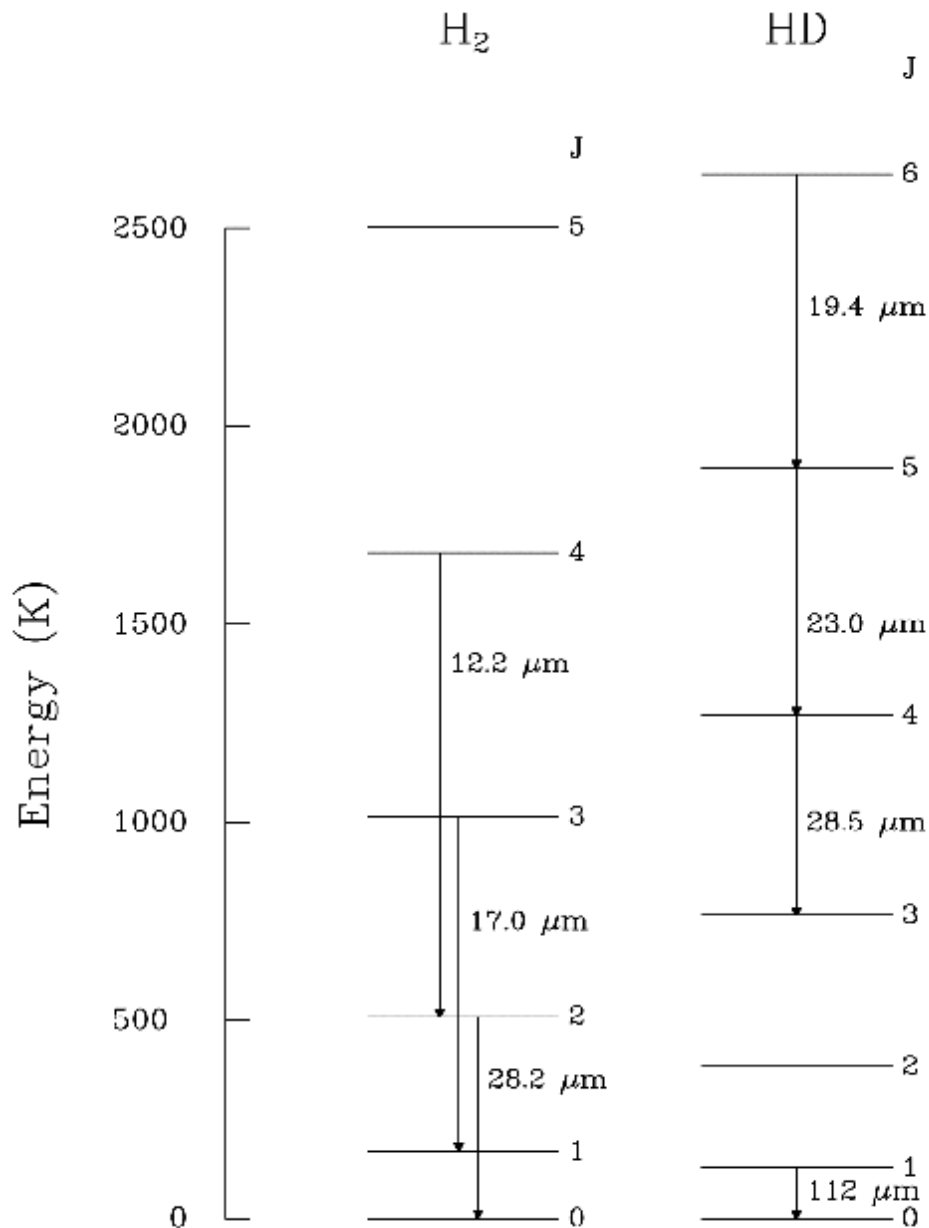


Figure 3. Energy level diagram of the H₂ and HD molecules, illustrating the fundamental pure rotational transitions

Gas-phase vibrational bands: Fundamental vibrational transitions of key molecules such as H₂O, CH₄, C₂H₂, HCN and CO₂ occur at 6.0, 7.7, 13.7, 14.0 and 15.0 μm. Symmetric molecules like CH₄ and C₂H₂ have no dipole moment and cannot be observed through rotational transitions at millimeter wavelengths. CO₂ and H₂O are so abundant in the Earth's atmosphere that they can only be detected from space. In addition to its importance in organic chemistry, CH₄ is also an excellent diagnostic of the atmospheres of brown dwarfs and giant exo-planets (Burrows et al. 1997).

Red-shifted bands: For objects at high redshifts, the features discussed above are shifted further into the mid-infrared wavelength range, and the potential of NGST to detect these lines in distant galaxies is mostly limited by the available wavelength range rather than the sensitivity. For example, the strong [Ne II] 12.8 μm line can be observed for $z < 1.4$, whereas the 6.2 μm PAH band is available for $z < 3.8$. Strong near-infrared bands such as Bracket-gamma can be searched up to $z \sim 12$, whereas H_α enters the mid-infrared range at $z > 6.6$.

The features and science discussed above and in [section II.2–9](#) lead to the desired instrumental characteristics summarized in [Table 2](#). A brief summary of the arguments for medium spectral resolution and integral field spectroscopy is given below.

Need for medium spectral resolution: A resolving power $R = \lambda/\Delta(\lambda) \sim 2000\text{--}3000$ is required because:

- (i) the ro-vibrational bands of gas-phase molecules become apparent only at $R \geq 2000$ (see [Figure 4](#));
- (ii) sub-structure in the solid-state bands is an important diagnostic tool and requires at least $R > 1000$. The PAH 7.7 μm band, which separates into at least 5 independent components at $R = 2000$, is a case in point. Also, many solid-state bands overlap at longer wavelengths and cannot be distinguished at $R < 1500$;
- (iii) detection of intrinsically weak and unresolved lines such as the H_2 S(0) and S(1) lines on top of strong mid-infrared dust continuum emission requires $R \sim 3000$ to obtain sufficient line/continuum ratio;
- (iv) the kinematics of galaxies (e.g., stellar mass determinations from the red-shifted CO 2.3 μm band) and outflows from protostars require velocity resolutions of $\sim 100 \text{ km s}^{-1}$, corresponding to $R \sim 3000$.

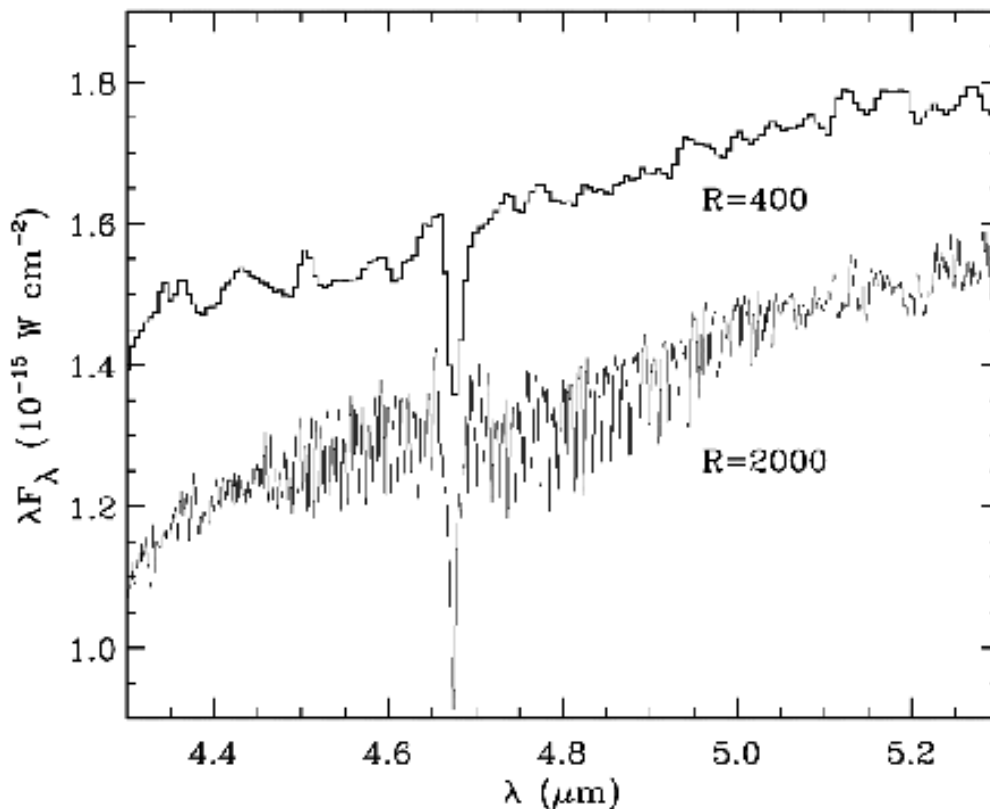


Figure 4. ISO-SWS spectra toward the young stellar object Elias 29 in the region of the CO vibrational band at $R = 400$ and 2000 . At $R = 400$, solid CO at $4.67 \mu\text{m}$ is detected, but the intrinsically much narrower lines of gas-phase CO between 4.5 and $5 \mu\text{m}$ only become visible at $R = 2000$, illustrating the need for medium resolution spectroscopy (Boogert 1999).

Case for integral field spectroscopy: While a conventional long-slit spectrometer is a minimum requirement for the NGST mid-infrared spectrometer, an integral field unit (in which a spectrum is obtained at each pixel in a two-dimensional array) would provide a much more powerful instrument for addressing the scientific problems. From limited ISO imaging, it is clear that many objects which appear spherical or axi-symmetric at optical wavelengths are highly asymmetric and 'blobby' at mid-infrared wavelengths. For example, in the nuclei of galaxies, PAHs and ionic lines have very different off-center distributions which would be missed in a single long-slit spectrometer setting (e.g. Le Flocc'h et al. 2001). Nearby protoplanetary disks often have a clumpy asymmetric distribution (e.g., Greaves et al. 1998). The sizes of these objects are typically a few arcsec in radius. Thus, a long-slit spectrometer covering $\sim 1'$ would be a very inefficient use of the array, whereas an integral field unit covering $\sim 4'' \times 4''$ would be well tailored to the science.

II.2. Obscured star formation in galaxies

The major science goal of NGST is to trace the star-formation history of the universe. It is now becoming clear that this is not a gradual process, but that most galaxies undergo bursts of intense star formation during their evolution. Extreme starbursts in distant high redshift galaxies may be responsible for much of the stellar populations of present-day galaxies. Remarkably, such starbursts are totally dust-enshrouded, and emit most their energy in the mid-infrared. Less extreme starbursts occur during the evolution of galaxies, often as the result of interactions with other galaxies. During these episodes, galaxies evolve rapidly in stellar content, in gas content, in spectrophotometric properties, in metallicity, in luminosity, and often also in morphology. Starbursts are therefore a fundamental driver of the evolution of the galaxy population, and mid-infrared observations are a key to their study (Genzel & Cesarsky 2000).

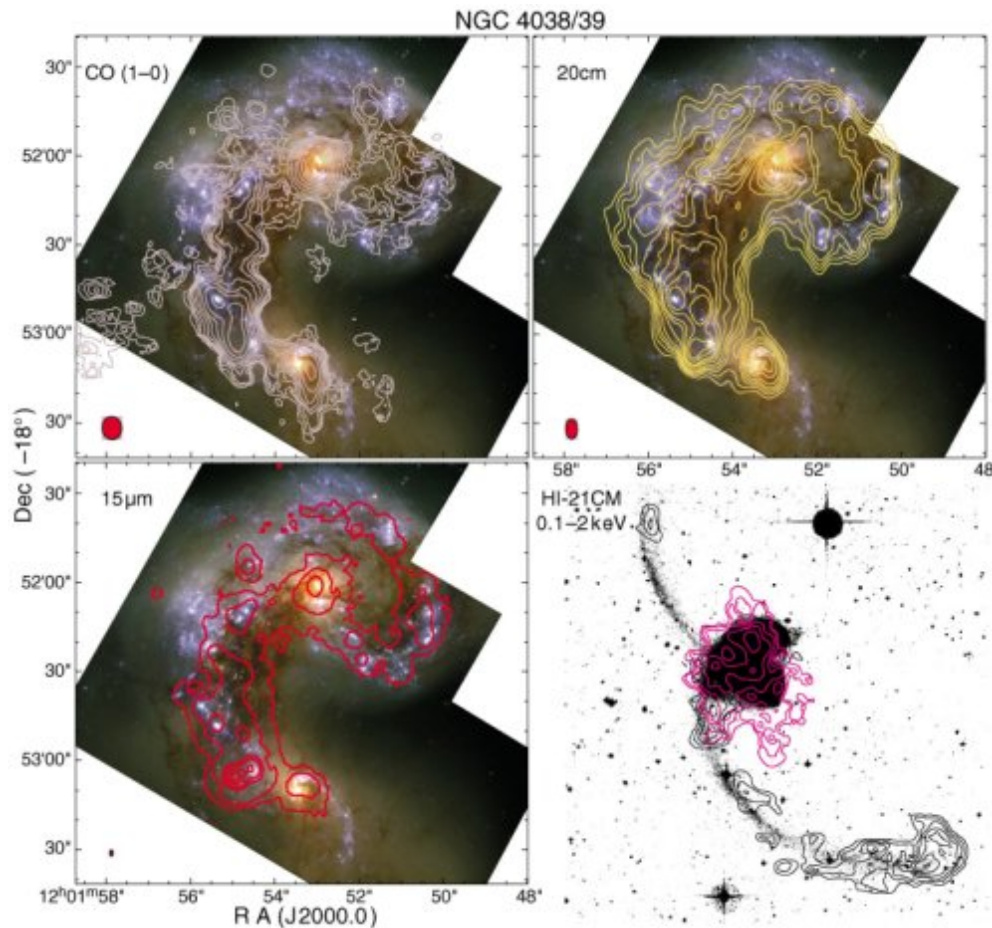


Figure 5. Various tracers in the NGC4038-4039 system (the "Antennae"). In the lower right frame the large-scale structure of the system is shown with X-ray (red) and H ~ I (black) contours superposed. The other 3 frames show the central 10 kpc of the merger. The underlying HST optical color picture reveals numerous young blue globular clusters, located mainly in an extended arm around the northern galaxy. However, the 15 μm image from ISOCAM (contours in lower left panel, Mirabel et al.1998) shows that the most intense star formation occurs in an optically obscured region where the disks interact. One remarkable cluster in the south-east region generates 15% of the total luminosity but is optically invisible. The present 15 μm image has 6'' resolution, as have the CO and radio continuum images shown in the other panels. NGST will produce imaging spectroscopy at a factor of 10 better spatial resolution.

At low redshift, the most extreme starbursts are found in mergers of gas-rich galaxies, where the dissipative gas components quickly sink to the center of the potential well, resulting in an intense burst of star formation. The ultraluminous infrared galaxies discovered by IRAS are a manifestation of this phenomenon and approach quasar-like luminosities up to $10^{14} L_{\text{Sun}}$, which is almost entirely emerging in the infrared regime. Based on these high luminosities, it has been suggested that powerful active nuclei and black holes are born in the obscured cores of gas-rich mergers.

A dramatic illustration of this effect is found in the nearby merging system NGC 4038-4039 (the "Antennae"). Here HST has produced spectacular images of the optical emission in the remnant host galaxies (see [Figure 5](#)), revealing numerous compact young star clusters. These sources represent young globular clusters formed as a result of the merger event. However, mid-infrared images obtained with the camera on ISO, ISOCAM, show that most of the star formation takes place in an optically obscured region where the two disks interact directly. One spectacular star cluster in this region accounts for more than 15% of the total luminosity, yet is totally invisible optically (Mirabel et al.

1998). High spatial resolution mid-infrared (10–30 μm) data will thus be needed to study the true, obscured, star formation properties of these rapidly evolving systems. Starburst phenomena occur even in our nearest neighbours (the Magellanic Clouds), as well as in other nearby galaxies such as M 33. Well-developed nuclear starbursts are found in very nearby spirals such as NGC 253, NGC 1808 and M 82. The availability of such local "laboratories" that can be studied in detail as templates for more distant sources makes this field an important science goal for NGST. The capabilities of NGST to probe the hot dust emission ideally complement those at longer wavelengths provided by Herschel and ALMA: whereas the hot dust probes violent (star formation) activity, ALMA and Herschel trace the cool dust, representing the pre-stellar material in galaxies.

The key role of the NGST mid-infrared instrument will be in spectroscopy in the 5–30 μm region. The numerous bright forbidden fine-structure lines of abundant ions (see [Table 3](#)) are excellent diagnostics of local kinetic temperatures and gas densities, and of the temperature of the exciting radiation field. The latter is related to the range of stellar masses present in the galaxy, the so-called Initial Mass Function (IMF). PAH features are also unique tracers of starbursts. Multi-line spectra can be used to separate the starburst and active nucleus as the power source. The potential of this approach has been demonstrated with (spatially unresolved) ISO spectra of nearby (up to $z \sim 0.1$) ultraluminous infrared galaxies (e.g., Genzel et al. 1998, Lutz et al. 1998, see [Figure 6](#)). While this work forms one of the principal heritages of the ISO mission, it also highlights the most outstanding questions in this field. For instance, many ultraluminous infrared galaxies contain an extreme starburst as well as an active nucleus (AGN) powered by a black hole. Does the occurrence of an extreme starburst trigger the formation of an AGN? How does this depend on the parameters of the starburst? Do globular clusters form in these immense compact star clusters? ISO did not have the spatial resolution required to separate these components, but NGST can provide spatially resolved information and probe much more distant galaxies.

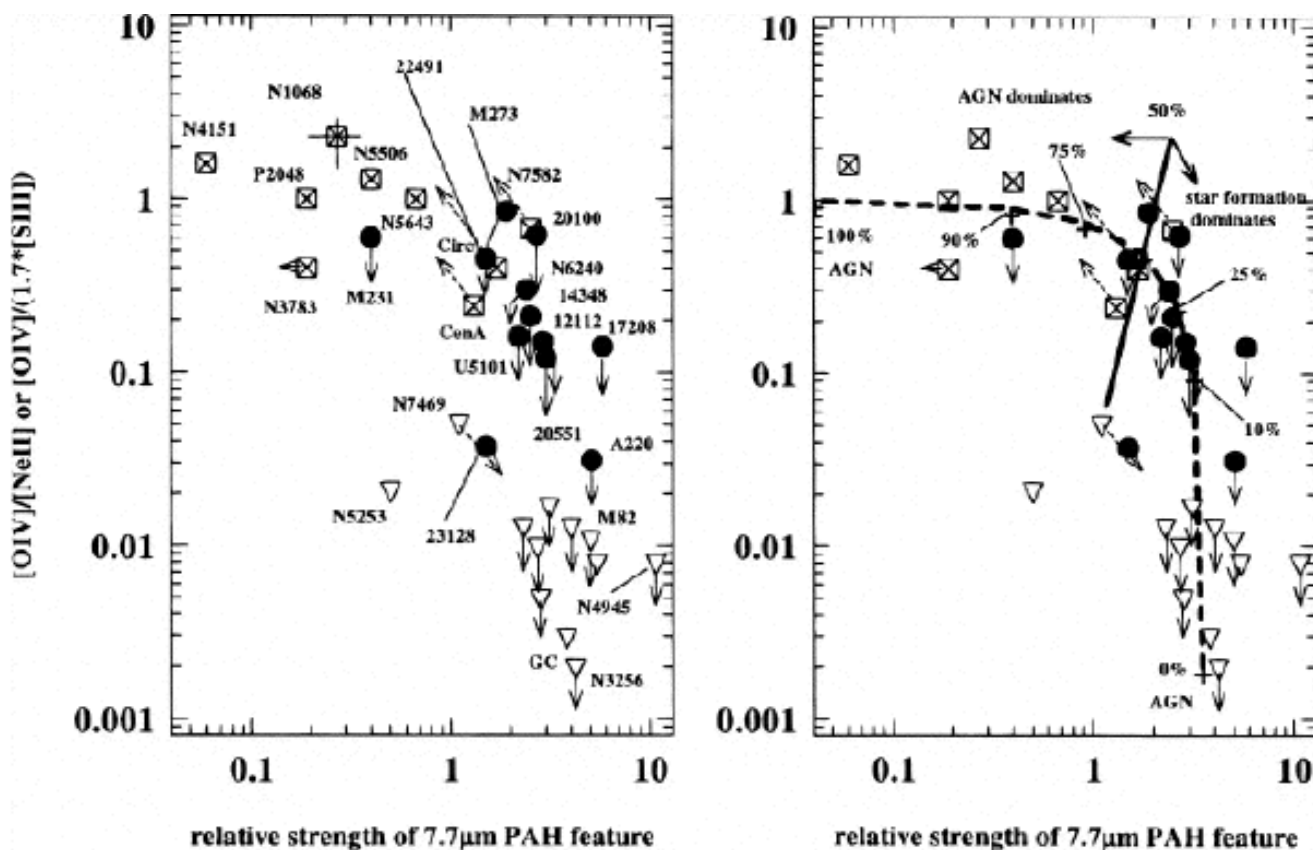


Figure 6. Diagnostic diagram showing the extinction-corrected 25.9 μm [O IV]/12.8 μm [Ne II] line ratios as functions of the strengths of the 7.7 μm PAH feature. Starburst galaxies are marked as open triangles, ultraluminous galaxies as filled circles and AGNs as crossed triangles. In the left figure, the individual galaxies are labeled. In the right figure, the areas of the diagram dominated by star formation and by AGNs are indicated (Genzel et al. 1998)

These projects require spectroscopy at $R \sim 3000$ in the 10–30 μm range, at the spatial resolution provided by NGST. Since the diagnostic lines are the major cooling lines for active massive star-forming regions, they are very luminous and detectable with NGST out to the redshifts where they shift out of the spectrometer passband. For instance, the very moderate starburst galaxy M 82 would be detectable in the [NeII] 12.8 μm line out to $z = 1.3$ (where the line shifts beyond 30 μm) at the 20-sigma level in only 1 hour for a 6.5m NGST with a 50 K focal plane. The Milky Way would be detectable out to the same redshift to the 5-sigma level in 1 hour under the same assumptions. Spatially, a 3 kpc starburst ring surrounding an AGN, such as that of the well-known nearby active galaxy NGC 1068 could be separated from the nucleus for galaxies out to 50 Mpc with NGST.

II.3. The high-redshift universe

Without observing the universe at wavelengths above 5 μm , NGST would miss much of the cosmic star formation history. Several independent observations show that most of the star formation taking place in early, distant galaxies is dust-enshrouded (Blain et al. 1999, Chary & Elbaz 2001). A result of paramount importance is the spectrum of the integrated extragalactic background, where the power in the infrared part due to re-radiation of absorbed starlight by dust exceeds the direct optical starlight by about a factor of 2 (Dwek et al. 1998, Gispert et al. 2000). Because at low redshifts the integrated infrared light is only $\sim 30\%$ of the optical light, this implies that the universe was much more obscured at high redshift than it is now. Quantitatively, an increase in infrared energy production out to $z \sim 2$ by a factor 30 is implied, and the infrared energy production should remain constant from $z = 2$ out to at least $z = 5$. Thus, star formation rates at high z derived from optical data alone will be greatly underestimated.

ISOCAM has lifted the tip of the veil in this spectral region. Deep ISOCAM images of the Hubble Deep Field South – one of the deepest images ever taken with HST – reveal typically 60 times fewer galaxies per unit area than HST, but these few galaxies produce at least a third of the integrated optical light (see [Figure 7](#)). Clear evidence for an increase in the infrared number counts is seen at the faint end, indicative of this new dusty population of galaxies at $z > 0.2$ (Elbaz et al. 1999). Interestingly, most ISOCAM-detected galaxies have optical/near-infrared counterparts that have totally normal optical colors; thus, it would not be possible to select these galaxies from optical/near-infrared data alone.

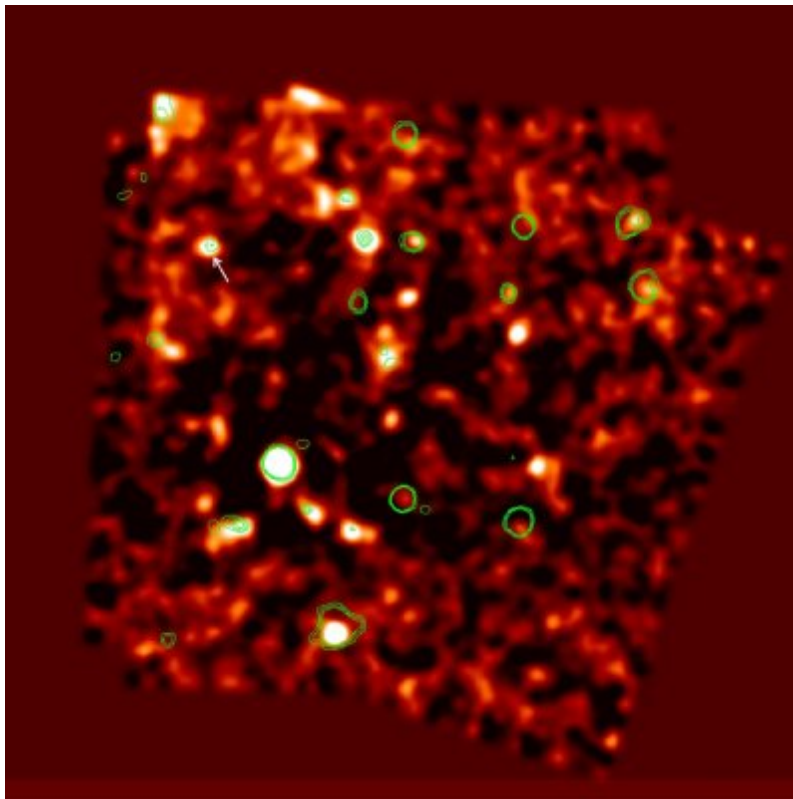


Figure 7. ISOCAM 15 μm image (color, 7' x 7') of the Hubble Deep Field South (HDF-S) WFPC2 field, with contours of the 6.7 μm image superposed (Oliver et al. 2001). This is one of the deepest mid-infrared images to date. The objects seen at mid-infrared wavelengths, in particular that indicated with the white arrow, are inconspicuous on the optical HDF-S data. The objects studied spectroscopically so far are classified as dusty starburst galaxies with redshifts up to $z \sim 1.3$. NGST will take the study of distant starburst galaxies out to much higher z .

A key NGST program beyond 5 μm will be the identification of this new population of galaxies accounting for most of the cosmic star formation through their dust emission. The mid-infrared spectra of dusty galaxies are dominated by deep silicate and ice absorption features and broad emission features attributed to PAHs, which are detectable out to high z . A modest $1 \times 10^{11} L_{\text{Sun}}$ starburst galaxy would be detectable out to $z \sim 3.5$ in the 6.7 μm band at 10 σ in 3 hours.

For a 6.5m NGST, the confusion limit at 25 μm is at 5×10^5 sources per deg^2 , which is very close to the optical source density in the Hubble Deep Field: 1×10^6 per deg^2 . Current infrared source population models indicate that this source density is reached at the 2 μJy flux density level at $\lambda = 25 \mu\text{m}$, which takes approximately 100 hours of NGST time. While SIRTf will make efficient large area surveys, its impact

will be significantly limited by confusion in the 8 times larger beam.

Mid-infrared observations also offer the unique opportunity of sampling the rest-frame $2\ \mu\text{m}$ region at $z > 2$, which is dominated by an evolved stellar population with mean age $>50\text{--}100\ \text{Myr}$ that cannot be isolated at shorter wavelengths, but which would trace a previous episode of star formation. For example, the masses of the so-called Lyman break-galaxies at $z \sim 3$ are very uncertain since it is not known whether or not an older underlying stellar population is present (Papovich et al. 2001). NGST will resolve the ambiguity between age and reddening which plagues the analysis of near-infrared colors. Moreover, spectroscopy of the CO band heads at rest-frame $2.3\ \mu\text{m}$ will provide a measurement of the velocity dispersions and hence dynamical masses of early spheroids. This will take the study of the cosmic star formation history from the measurement of light to the measurement of mass, which will be a major breakthrough. Medium spectral resolution observations at $R \sim 3000$ are essential for this project.

The $\lambda > 5\ \mu\text{m}$ region also gives access to the most important nebular lines at the highest redshifts, in particular H_{α} at $z > 6.6$. This redshift regime corresponds to the epoch of recombination, where cosmic first light ionizes the gaseous universe. The H_{α} line is crucially important since (unlike Ly_{α}) it is not affected by resonant scattering and therefore forms a direct and quantitative probe of the ionizing flux. The star formation rate of the first galaxies can thus be directly measured using redshifted H_{α} , and any dust extinction can be corrected using the H_{α}/H_{β} line ratio. Since the epoch of cosmic first light is one of the cornerstone science targets of the NGST, this application is of key importance to the mission (Haiman & Loeb 1998, Ciardi & Ferrara 2001).

II.4. Star formation

The processes by which stars, protoplanetary disks and planets are formed remain poorly understood. NGST will play a vital role in this area, in concert with complementary facilities such as ALMA and Herschel. The tremendous sensitivity of NGST at mid-infrared wavelengths is essential because protostars and disks are relatively cool with huge dust extinctions, so that they are impossible to penetrate at shorter wavelengths. The high spatial resolution of NGST is needed to zoom in on protostellar disk formation, to image gaps in disks around more mature pre-main sequence stars and to detect faint brown dwarfs and extrasolar giant planets close to their bright parent stars. Because star- and planet formation is accompanied by huge changes in the physical conditions, with densities ranging 10^4 to $10^{13}\ \text{cm}^{-3}$ and temperatures from 10 to 10,000 K, there are a wealth of atomic and molecular lines available with which to unravel the physical structure and evolution. Moreover, these lines can be used to trace the chemical composition of gas and dust through the various stages of the star formation process, thus providing an inventory of the building blocks available for new solar systems (Figure 8).

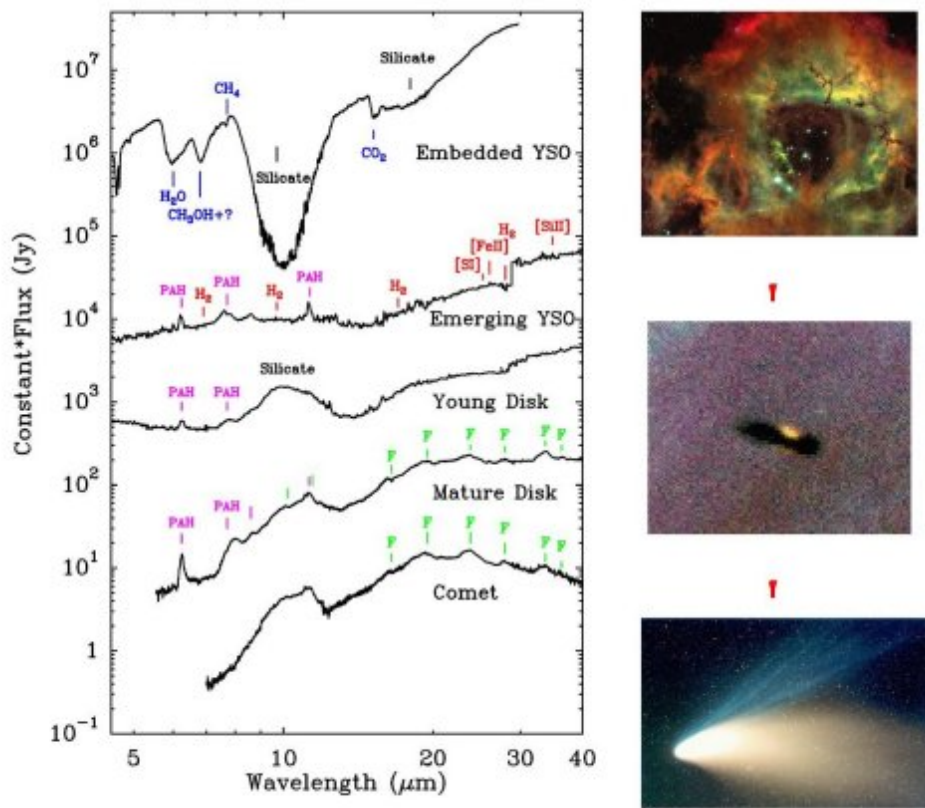


Figure 8. The ISO-SWS mid-infrared spectra of newly-formed stars in different stages of formation and circumstellar disks (Gibb et al. 2000, van den Ancker et al. 2000, Malfait et al. 1998). From top to bottom – in a rough evolutionary sequence – the spectra change from dominated by solid state absorption features and gas (shock) emission lines, to featureless, to PAH features and PDR lines, to amorphous and crystalline silicates (F = Forsterite) with H ~ I recombination lines. The ISO-SWS spectrum of comet Hale-Bopp is shown for comparison (Crovisier et al. 1997).

Deeply-embedded protostars: Mid-infrared observations with NGST will be particularly powerful to provide insight into the physical processes occurring in the deeply embedded protostellar phase when the star is still being assembled through accretion of material from the circumstellar disk. The fragmentation of the collapsing cloud into binary or multiple star systems and the formation of the disk itself are key questions, which can likely only be addressed properly through combined NGST mid-infrared and ALMA data. Mid-infrared continuum images at $>20\ \mu\text{m}$ probe the warm part of the accretion disk and the inner envelope, constraining the geometry and the elusive mass infall rate (see simulations in Serabyn et al. 1999). Imaging in different spectral features such as the H_2 pure rotational lines and the [S I] $25.2\ \mu\text{m}$ line probe the physics of the accretion shock at the disk surface, as well as the interaction of the outflow with the inner envelope as it starts to clear the surroundings (van den Ancker et al. 2000, Figure 8). Periodic structures in the outflow jets may be used to trace the recent accretion history of the central protostar. The PAH features track the importance of ultraviolet radiation in dispersing the envelope. Together, such data can trace the protostellar evolution from the earliest collapse to the phase where the young stars emerge from their natal cocoons.

The high sensitivity and spatial resolution of NGST are essential for these projects, since the youngest protostars have mid-infrared continuum fluxes of less than a mJy (see Fig. 2 in André et al. 2000) and the disks have sizes of at most a few arcsec (a few hundred AU) for typical distances of 150–300 pc. The SIRTf legacy program of Evans et al. (2001) (including van Dishoeck as co-I) will detect all protostars with luminosities down to $1.5 \times 10^{-3} L_{\text{Sun}}$ as well as young stars and substellar objects down to $5 M_{\text{J}}$ in five nearby molecular clouds, providing a prime database for NGST high-resolution imaging and spectroscopy follow-up.

Massive young stars: More distant, massive protostars are also prime targets for NGST mid-infrared observations. Little is known about the earliest stages of massive stars, for example whether their formation is accompanied by circumstellar disks as in the case of low-mass stars. Also, traditional models of massive star formation through the collapse of a single cloud core are being challenged by alternative models of merging of lower-mass stars in the central potential of very dense clusters (Stahler et al. 2000). Since this latter mechanism would occur in the deeply embedded phase, only sensitive high spatial resolution NGST observations, combined with ALMA data, will be able to resolve such clusters of ~ 10 – 100 low-mass stars crammed into a ~ 1000 AU region out to a few kpc. Once formed, the massive young stars enter the ultra-compact H II region phase, in which they ionize the surrounding gas. A circumstellar disk consisting of hot dust and gas (~ 4000 K) may still exist in regions shielded from the intense ultraviolet radiation of the central star (Hanson et al. 1997, Lenorzer et al. 2001). High-spatial resolution infrared spectra are required to study the distribution and physical nature of this hot dust and gas and confirm the presence of disks.

II.5. Protoplanetary disks

One of the most exciting developments in astrophysics in the last decade has been the definite detection of extrasolar planets around nearby stars via the radial velocity technique (Mayor & Queloz 1995, Marcy & Butler 1996). More than 60 of these exo-planets are now known, showing that planet formation is common and reviving age-old questions about their formation. The planets are thought to have originated in the disks or 'pre-solar nebulae' around young stars, first postulated by Kant in 1755 for the origin of our solar system. The existence of such disks was inferred from pioneering infrared and millimeter observations in the early 1990's and it is now commonly accepted that more than 50% of young stars have disks (see Beckwith & Sargent 1996 for a review). Disks are also beautifully seen as silhouettes against a bright background in HST optical (e.g., McCaughrean & O'Dell 1996, Burrows et al. 1996), and near-infrared images (e.g., Padgett et al. 1999). The sizes of the disks are typically a few hundred AU, comparable to that of our own solar system.

Toward the end of the star formation process, the accretion of matter onto the star through the disk stops and the dust in the disk begins to coagulate to form larger and larger bodies, becoming the seeds for planetesimal formation. Once these are self-gravitating, they accrete even faster and may develop into proto-planets. However, a detailed understanding of the processes by which disks turn into planets, the time scales involved, the frequency of planet formation and its dependence on external influences, and the evolution and dissipation of the primordial gas and dust in the disk, is still lacking. The fact that none of the known exo-planetary systems resembles our own solar system indicates that existing theories need to be revised (e.g. Artymowicz 2001). The combination of NGST mid-infrared and ALMA submillimeter data will allow major steps forward in our understanding of protoplanetary disk evolution.

Young massive disks: The gas-rich disks seen around pre-main sequence T Tauri and Herbig Ae stars with ages of a few Myr have gas + dust masses of $0.01 M_{\text{Sun}}$, similar to that of our primitive solar nebula. Once accretion stops and the dust starts to coagulate, both the geometry and composition of the disk undergo substantial changes. These changes can be studied best in the mid-infrared spectral region, since at these wavelengths the inner disk, where planet formation is expected to occur, dominates the spectrum. In particular, changes in dust scale height affect the strength of the mid-infrared flux emerging from the disk, while structural modifications in the dust grains result in mineral formation traced by mid-infrared spectra (e.g. Chiang et al. 2001, Meeus et al. 2001, Dullemond et al. 2002, see [section II.7](#)). The possibility of obtaining spatially resolved images with NGST and ALMA down to ~ 10 AU will allow not only the dust settling, but also the relative settling of the dust versus the gas in gas-rich disks to be determined and the earliest stages of planetesimal formation to be followed up to roughly millimeter sizes. Indirect evidence for planet formation will be provided by observations of gaps in disks, where an unseen giant planet has cleared out a ring of material. The power of mid-infrared data for these studies was demonstrated by Koerner et al. (1998) for HR4796A. For the brightest systems in the nearest star-forming regions, MIDI on the VLTI can zoom in even closer and detect the warm material in the 1–10 AU range.

Most disks have been studied through their dust emission, but 99% of the mass is in H_2 gas. Not only does this gas affect the dynamics of the dust, but it is also the principal ingredient for giant Jovian planet formation. It has recently become clear that CO is not a good tracer of the gas in disks due to the combined effects of photodissociation in the surface layers and freeze out in the cold midplane (van Zadelhoff et al. 2001, Aikawa et al. 2001). In contrast, H_2 traces the bulk of the warm gas at $T > 50$ K directly. The ISO-SWS provided the first opportunity to search for the principal H_2 $J = 2-0$ S(0) and $3-1$ S(1) lines at 28 and 17 μm , and detected lines not only from disks around young pre-main sequence stars (Thi et al. 1999), but also tentatively from disks around 10–20 Myr old stars such as Beta Pictoris (Thi et al. 2001a,b, see [Figure 9](#)). This would indicate that these latter objects are better thought of as the final stages of gas-rich accretion disks. The time scale over which this gas clearing occurs and the mechanisms by which it operates are critical to both planetary formation and migration models. Currently there is still no consensus whether giant planets originate through the formation of a rock-ice core followed by gravitational gas accretion or by instabilities in the outer disk and fragmentation. Combined spatially resolved observations of both the dust and H_2 as functions of age over the 1–100 Myr range will be powerful tools to distinguish between these models.

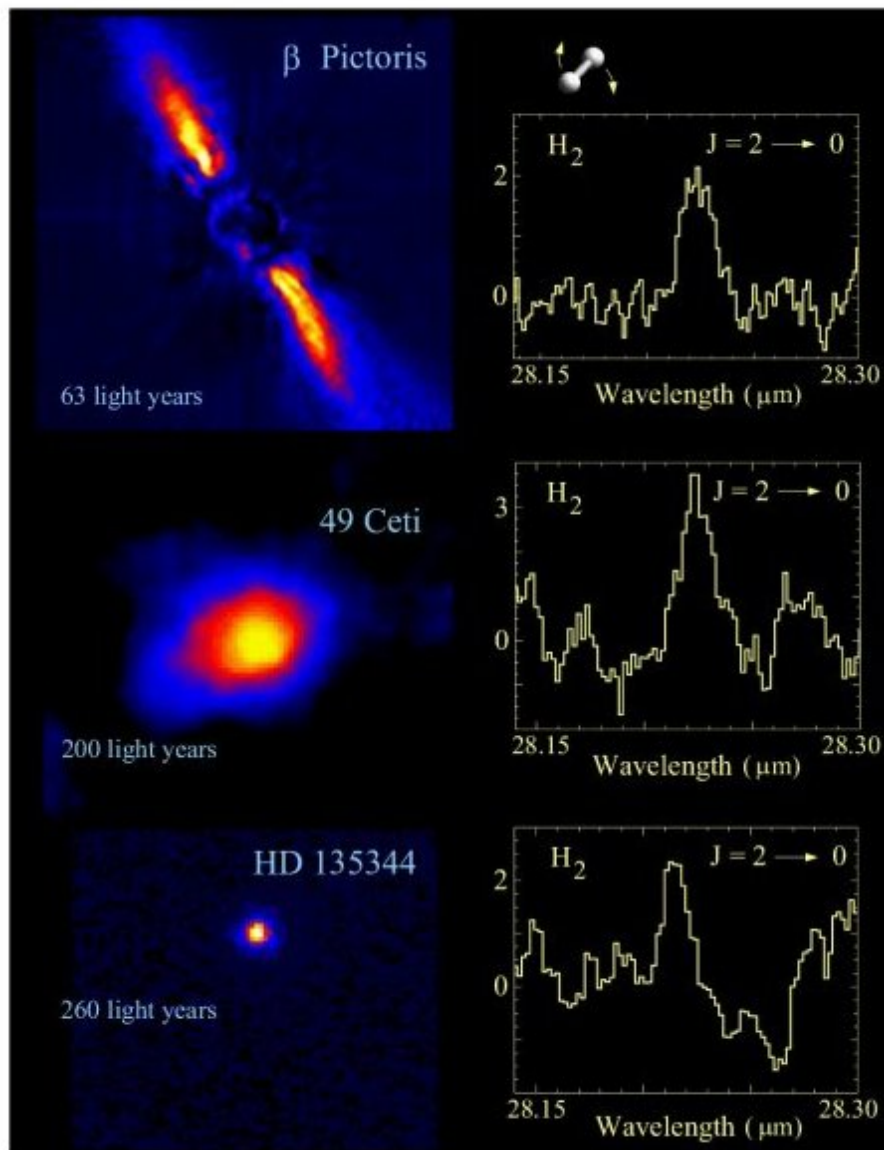


Figure 9. ISO-SWS observations of H₂ toward the 'debris' disks around Beta Pictoris, 49 Ceti and HD 135344 (Thi et al. 2001a,b). The Beta Pictoris 1.25 μm scattered light image is based on Mouillet et al. (1997). The 20 μm thermal emission image of 49 Ceti is from Koerner (priv. comm.) and that at 12 μm of HD 135344 from Blake & Kessler (priv. comm.).

NGST will be sensitive to gas with masses of 10^{-3} – $10^{-7} M_{\text{Sun}}$ at $T_{\text{gas}} = 50$ – 200 K (see Figure 12 of van Dishoeck 2000). The high spectral ($R \sim 3000$) and spatial resolution of the NGST mid-infrared instrument is essential for this project: even though SIRTf will attempt to observe H₂ from disks, the low line/continuum ratio at $R = 600$ will prevent detection in most cases.

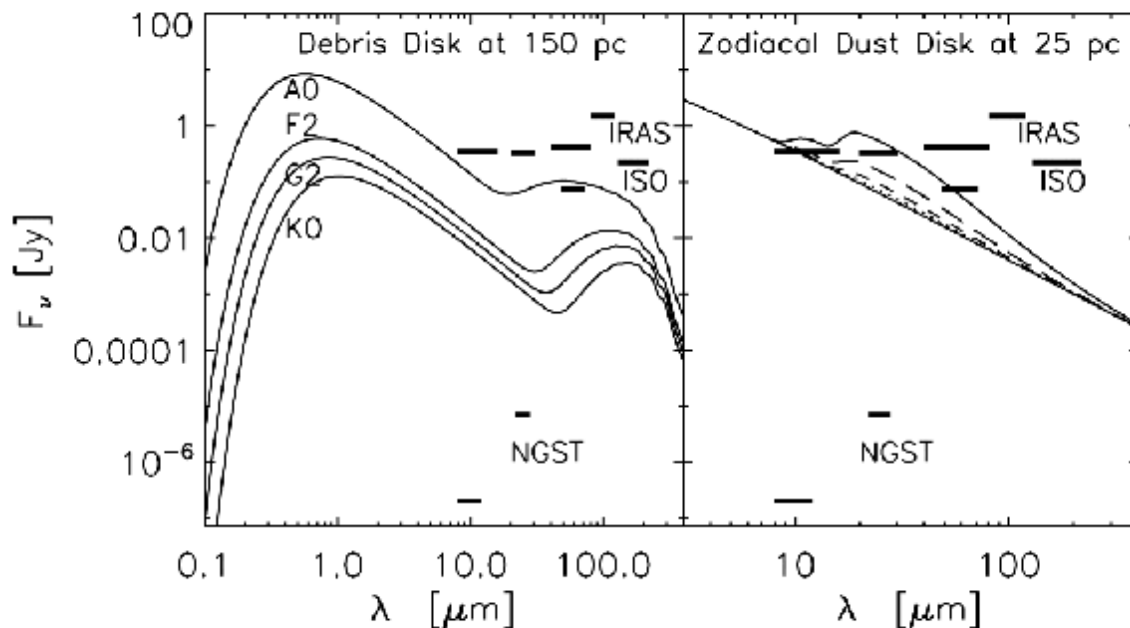


Figure 10. Left: Flux density distributions for model debris disks around stars of various spectral types in nearby star-forming regions. The models assume $0.1 M_{\text{Moon}}$ of $30\text{-}\mu\text{m}$ -sized dust grains in a zone extending from 30 to 60 AU radius, using the Draine & Lee (1984) dust properties. The NGST 5-sigma sensitivity in 0.7 hr is indicated. Right: Flux density distributions for zodiacal dust ($1\text{-}\mu\text{m}$ -sized grains between 3–5 AU) around a G-type star at 25 pc. The masses are 10^{-5} , 3×10^{-5} , 10^{-4} and $5 \times 10^{-4} M_{\text{Moon}}$ (Dominik, priv. comm.).

Debris disks: Current near-infrared surveys for excess emission indicate that the massive disks disappear in a few Myr (Haisch et al. 2001). However, these data are only sensitive to very warm dust close to the star. Longer wavelength observations are needed to trace the evolution of the bulk of the dust beyond the classical T Tauri stage. The SIRTf guaranteed and legacy programs of Meyer et al. and Evans et al. will survey several hundreds of young stars with ages ranging from a few to several hundred Myr, including weak-line T Tauri stars associated with the closest star-forming clouds (ages 1–20 Myr), X-ray bright young stars in the solar neighborhood for which accurate distances are known from Hipparcos (ages ~ 10 –100 Myr), and young main sequence stars in open clusters with age >30 Myr. Together, they will produce a phenomenal database for subsequent NGST spectral imaging of disk evolution around solar-type stars in the planet-forming phase. NGST can detect disks with only a fraction of a lunar mass throughout the solar neighborhood (see Figure 10).

Eventually, the original gas and dust in the disk will have dissipated and/or coagulated into larger bodies. The disk will then continue to evolve collisionally over a period of typically 400 Myr, resulting in the destruction of larger bodies and the production of new so-called 'debris' dust, first detected by IRAS (Aumann et al. 1984) and surveyed by ISO (Habing et al. 1999). A similar period of collisions occurred in the early solar system, as evidenced from, for example, the formation of the Moon and the impact record of asteroids on the Moon. The zodiacal dust in the inner regions of the solar system is the result of fairly recent collisions of asteroids in the asteroid belt, whereas a colder component resides in the Kuiper belt. Such exo-Kuiper belts have been imaged in a few cases at submillimeter wavelengths by SCUBA on the JCMT (Holland et al. 1998, Greaves et al. 1998), but those data are not sensitive to the warm inner solar system dust. Even though the zodiacal grains compose only a very small fraction of the mass in our solar system ($<10^{-10}$), they intercept and re-radiate effectively a fraction $\sim 10^{-7}$ of the Sun's energy and therefore account for the lion's share of its far-infrared radiation. Thus, even 4.5 Gyr after its formation, zodiacal dust provides the more readily detectable indirect evidence of a solar system like our own.

NGST will have the sensitivity to study the composition and geometry of exo-zodiacal dust near other stars in great detail (Figure 10). IRAS and ISO showed that $\sim 15\%$ of stars have more than 100 x the amount of cold dust in our own solar system, but these statistics are based on a small sample and limited entirely to the more massive A-type stars. NGST would allow solar-system levels of zodiacal dust to be detected around Sun-like stars out to distances of at least 25 pc. More importantly, its high spatial resolution will allow the disk to be distinguished from the stellar photospheric emission and the surrounding interstellar 'cirrus' emission. Knowledge about exo-zodiacal mid-infrared dust emission will also be essential for planning future missions such as IRSI-DARWIN and TPF, since a strong exo-zodiacal light component will severely restrict the possibilities to detect Earth-like planets in habitable zones.

II.6. Giant exo-planets and brown dwarfs

The primary goal for future space missions such as ESA's DARWIN/IRSI and NASA's TPF in the middle of the next decade is the direct detection of Earth-like planets and the probing of their atmospheres for signs of life. NGST will form an important bridge toward this aim, not only by enhancing our understanding of the mechanisms by which planets form from disks (see [section II.5](#)), but also by allowing detection and characterization of extrasolar giant planets and their atmospheres.

The spatial resolution and sensitivity of NGST will allow a direct spectroscopic detection of Jupiter-like giant planets in wide (>5 AU) orbits around the nearest stars (<10 pc). These observations are best done near 5 μm , where the molecular opacity in the outer atmosphere of a gas giant is low so that warm thermal emission can emerge. Searches for these objects may be carried out with a coronagraph in the NGST near-infrared camera, but a simple coronagraphic option in the mid-infrared camera is being considered as well. Once found, follow-up mid-infrared spectroscopy can characterize the planetary atmospheres and study their chemistry as a function of mass, age and temperature ([Figure 11](#)). With large enough statistics, such observations may also give insight into the formation history and possible migration of giant gas-rich planets. For instance, planets formed late in the evolution of the protoplanetary disk are expected to have less gas and a different composition.

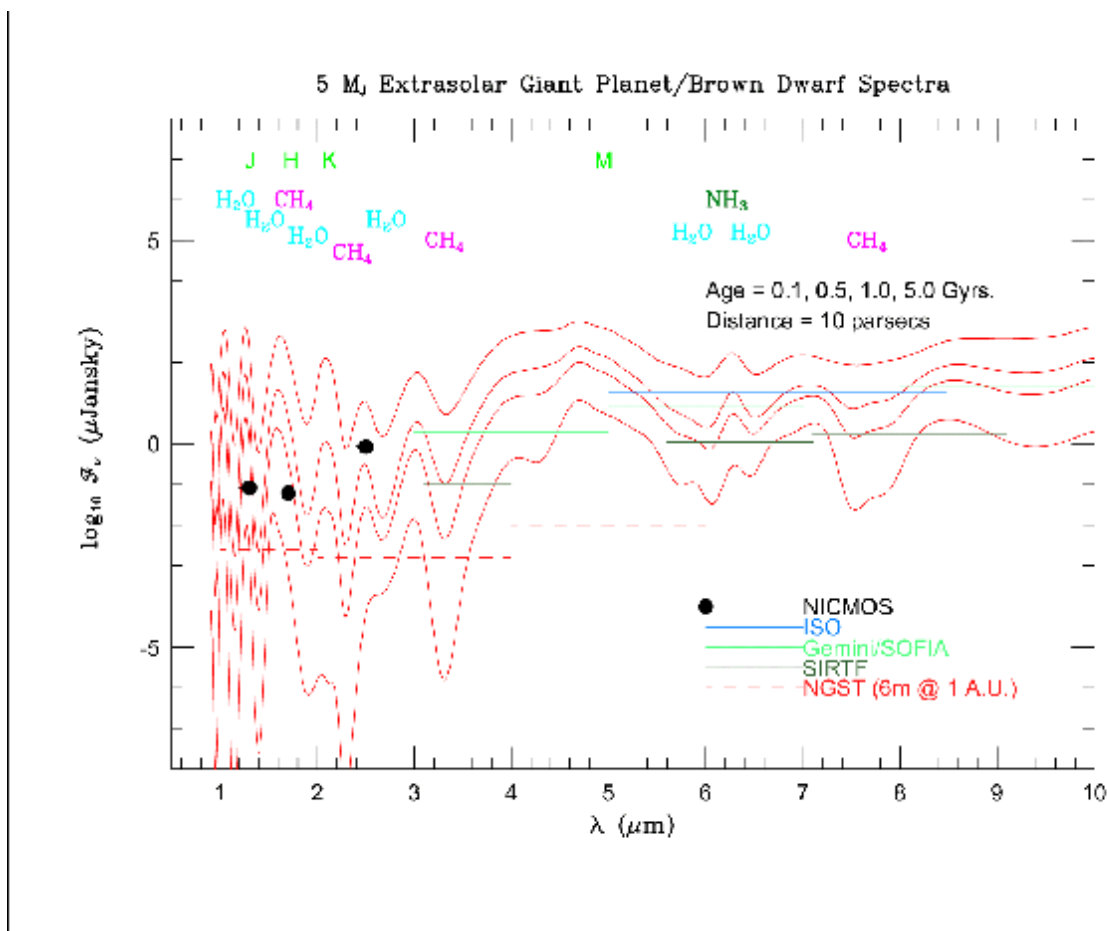


Figure 11. Model atmospheres of a $5 M_J$ exo-solar giant planet at a distance of 10 pc at different ages. Note the strong spectral evolution with time in the mid-infrared part of the spectrum. Only NGST has the sensitivity to follow this evolution for Jupiter-type objects (based on Burrows et al. 1997).

NGST will also be enormously powerful for studying other substellar objects such as brown dwarfs with masses in the $0.01\text{--}0.07 M_{\text{Sun}}$ range. Thanks to the 2MASS, DENIS and SLOAN surveys, more than a hundred of these objects have now been discovered (e.g., Kirkpatrick 2001), and ground-based surveys with large optical telescopes will pin down the initial mass function in this regime in young clusters. However, several questions can only be addressed by space-based mid-infrared imaging and spectroscopy. For example, are young brown dwarfs surrounded by their own disks during formation, i.e., do they indeed form as stars do, or do they form as companions to stars? Also, are their atmospheres dusty, i.e., can we see 10 μm silicate emission? Theoretical models predict significant changes in the atmospheric composition with age and mass, especially around 8 μm due to NH_3 formation (Burrows & Sharp 1999). SIRTf will provide a first glimpse of these

spectra, but lacks the sensitivity and spectral resolution for a proper survey.

II.7. Tracing the astrochemical evolution

Generations of low- and high-mass stars have converted the primordial hydrogen and helium into successively heavier elements including carbon, oxygen and nitrogen (see [section II.8](#)). These elements are mixed into the diffuse and dense interstellar medium and may eventually end up in the envelopes and disks around young stars. Tracing the lifecycle of the gas and dust from the pre-stellar cores to their eventual incorporation into planetary systems where they may be the stepping stone toward prebiotic molecules, is a major goal of astrochemistry and the new discipline of astrobiology (see reviews by van Dishoeck & Blake 1998, Waters 2000, Ehrenfreund & Charnley 2000, van Dishoeck & Tielens 2001).

In the cold quiescent clouds prior to star formation, gas-phase molecules collide with the grains and stick, forming icy mantles around the silicate cores. Indeed, this freeze-out is predicted to be so efficient that it has been a puzzle for decades why any gas-phase molecules are seen at all in cold regions. Recent indirect evidence based on near-infrared star counts and millimeter data suggests that the amount of depletion inside dense cores can be substantial, with more than 90% of the heavy elements (including oxygen and carbon) frozen out onto the grains (Lada et al. 1999, Kramer et al. 1999). NGST will be the first instrument capable of probing this depletion process directly, through near- and mid-infrared observations of solid-state absorption bands toward hundreds of background stars located behind dark clouds, providing "maps" of the freeze-out process.

The ices in the cold outer envelopes around protostars can be observed through medium-resolution absorption spectroscopy. In the earliest collapse stages, more of the heavy elements are frozen out and the chemical composition is modified through grain-surface reactions. As the surroundings are heated by the protostar, the ices gradually evaporate back into the gas phase ([Figure 4](#)). [Figure 8](#) includes the ISO-SWS mid-infrared spectrum toward the embedded massive protostar W33A, which is particularly rich in various (organic) features (Gibb et al. 2000). ISO has been able to obtain such high-quality spectra for only a dozen massive protostars with luminosities of 10^3 – $10^5 L_{\text{Sun}}$, but information on low-mass protostars is lacking almost entirely. Since SIRTf lacks the required spectral resolution, only NGST will be able to perform a complete census of solid-state material as it enters the planet-forming disks around solar-type stars.

The ice and gas-phase data also reveal the thermal and irradiation history of the protostellar envelope. The solid CO_2 bending mode at $15 \mu\text{m}$ is a particularly sensitive diagnostic of the ice environment, with a characteristic double-peaked structure appearing upon heating by the young star (Ehrenfreund et al. 1998, Gerakines et al. 1999). Other features, such as the OCN^- band at $4.62 \mu\text{m}$ and the unidentified $6.85 \mu\text{m}$ feature, are sensitive to ultraviolet irradiation (Schutte & Greenberg 1997, Schutte et al. 2001). Since the changes in the band profiles are irreversible, they record the cumulative events experienced during the protostellar phase such as FU-Orionis-type outbursts related to disk accretion. The analysis of the NGST data will greatly benefit from the involvement of the Raymond & Beverly Sackler/NOVA Laboratory for Astrophysics at Leiden.

Part of the gas and dust from the protostellar envelope will be incorporated into the circumstellar disk, where it can be further processed by ultraviolet radiation, X-rays and thermal processes. In the cold midplane, most molecules are expected to be frozen out on the grains and NGST will have the sensitivity to probe these ices in absorption against the star in edge-on geometries. Emission from gas-phase molecules such as H_2 , CO , CH_4 and C_2H_2 from the warm inner regions can be searched for at the highest spectra resolution.

The dominant spectral emission features from disks are expected to be due to PAHs, ices and silicates, both in amorphous and crystalline form. These dust particles are the building blocks of planets, asteroids and comets. Our solar system has a very rich mineralogy which holds the formation record of its solid bodies; examples are the olivines (one of the major constituents of the Earth's crust), silica, iron sulfide and carbonates. The latter material is linked to the presence of liquid water on large parent bodies. The minerals are believed to have played a key role in the formation of life on Earth through their ordered lattice structure. In contrast, interstellar clouds have so far revealed only a limited number of fairly simple materials such as amorphous silicates and carbon, demonstrating that substantial processing of the dust must occur as solar system planetesimals are formed. Grains can stick together, they can be heated by electric current discharges or by stellar radiation which alters their lattice structure, and gas-solid reactions can modify their chemical composition. Mid-infrared spectroscopy of protoplanetary disks with NGST can probe these changes and trace the formation of planetesimals and other solid bodies that would be undetectable directly due to their small radiating surfaces. In combination with laboratory light scattering experiments of cosmic dust analogues, both the composition and size of the dust particles can be established. Such light scattering measurements are being performed using the University of Amsterdam-NOVA/FOM-AMOLF light scattering experiment.

The ISO-SWS has allowed a first glimpse of the rich mid-infrared spectra of disks around pre-main sequence stars. Indeed, one of the major results is that solid-state evolution of grain minerals is observed (e.g., Malfait et al. 1998, Meeus et al. 2001). Some objects show only amorphous dust emission, whereas others have clear signatures of crystalline silicates and/or PAHs similar to those found in comets (see [Figure 8](#) and [front cover](#)). These variations appear related to the processes in grain coagulation, settling and thermal annealing in the disk

(Bouwman et al. 2001). The ISO-SWS did not have the sensitivity to probe disks around solar-type stars. SIRTf will provide the first data on lower-mass objects, but will be spatially unresolved and has the sensitivity to do only $R = 100$ spectroscopy on the more evolved debris disks. Only NGST will be able to follow the entire dust evolution in the 1–600 Myr range for Sun-like stars.

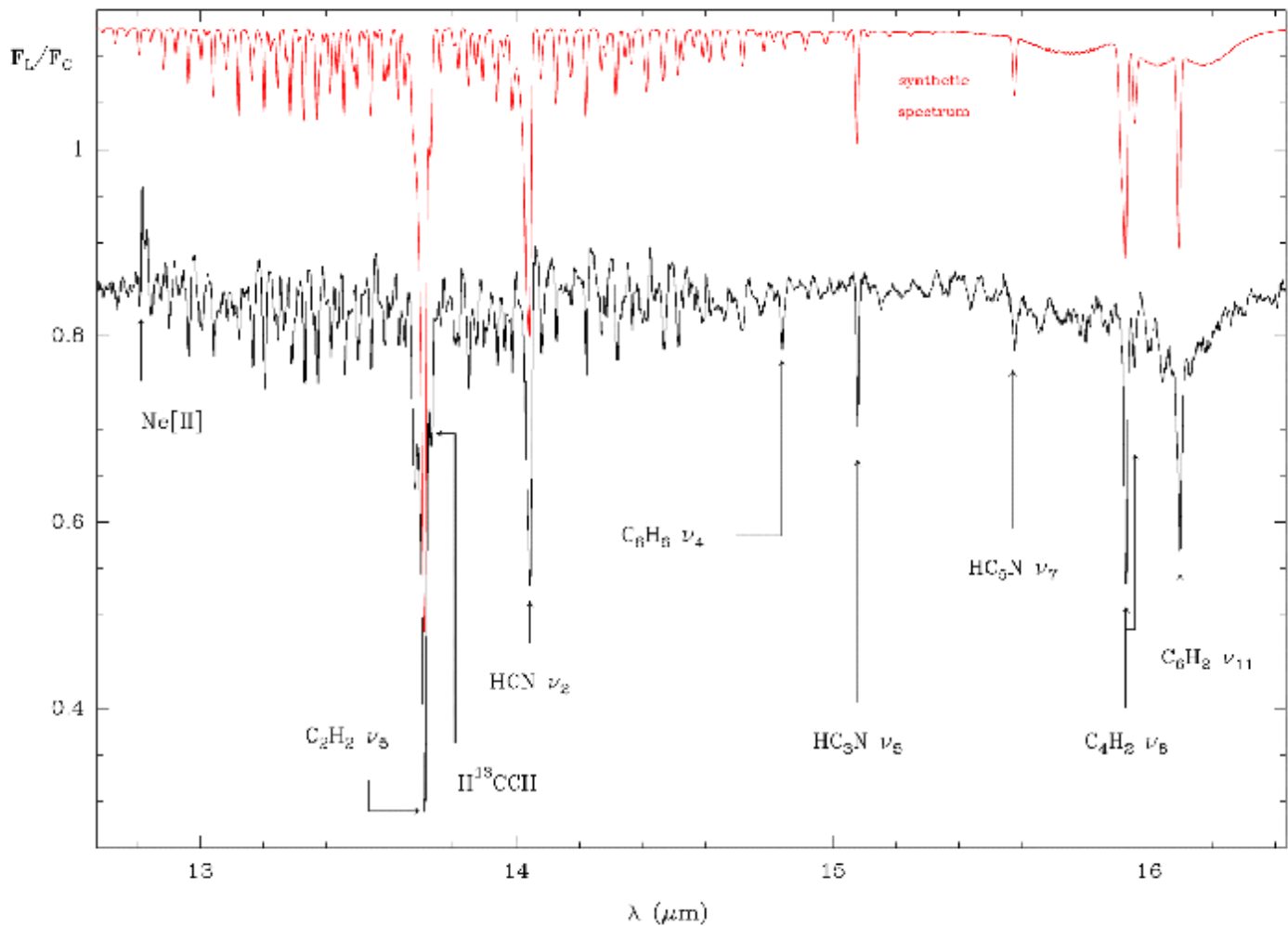


Figure 12. The 12–17 μm spectrum of CRL 618 – obtained by the SWS on ISO – illustrating the molecular complexity of AGB ejecta. The model (red) includes the ro-vibrational transitions of acetylenic chains (C_2H_2 and C_4H_2) and their nitrile derivatives (HC_3N , HC_5N), hydrogen cyanide, and benzene (C_6H_6) (Cernicharo et al. 2001.)

II.8. The death of low mass stars

Low mass stars such as the Sun ($<8 M_{\text{Sun}}$) end their lives by returning most of their mass to the interstellar medium in the form of a gentle wind (velocity $\sim 10 \text{ km s}^{-1}$) while evolving on the so-called Asymptotic Giant Branch (AGB). At that point, all of their hydrogen in the core has burned to helium during the main sequence stage of evolution, and subsequently to carbon and oxygen during the horizontal branch stage of evolution. The central core is then essentially a white dwarf surrounded by a large convective envelope. While these stars derive their energy from burning alternately hydrogen and helium in a shell around the core, stellar evolution during this stage is driven by mass loss from the star rather than nuclear burning. Eventually, when the whole envelope is lost, the central white dwarf will evolve rapidly to the blue and ionize and heat the previously ejected material. This will set it aglow, forming a planetary nebula. The dust and gas in the ejecta absorb much of the visible and near-infrared radiation from the star and reradiate it in the mid-infrared, so NGST is particularly well suited to study the death struggle of stars.

Studies of the mass loss during the AGB phase are important not only to study stellar evolution, but also because these stars dominate the mass budget of the interstellar medium. The gas in AGB winds consists largely of molecules ranging from the mundane H_2 and CO to the exotic HC_9N and PAHs. The ejecta from these stars are a major source of carbon as well as the source of all the s-process elements in the interstellar medium. Most of the heavy elements are returned to the interstellar medium in the form of small dust grains, which then form the building blocks of new stars and planets. Indeed, even in the heavily processed environment of the inner solar system, relic stardust grains have been recovered (Bernatowicz et al. 1996, Tielens 2001).

During this mass loss phase, the mid-infrared spectra of AGB stars are dominated by the vibrational signatures of the surrounding dust and gas. As an example, [Figure 12](#) shows a small portion of the infrared spectrum of the heavily enshrouded source, CRL 618, which has just left the AGB, illustrating the molecular richness of the envelope. The composition of the dust is set to a large extent by the elemental composition of the ejecta. If the star is oxygen-rich, silicates and oxides are formed. In carbon-rich ejecta, carbonaceous materials, such as carbides and hydrogenated amorphous carbon grains condense. The dust formed also depends on the density and temperature in the condensation zone. Hence, AGB stars and their descendants show a bewildering zoo of dust types. [Figure 13](#) illustrates the spectral richness of stardust. While most spectra follow this dichotomy of O- versus C-rich dust, an increasing number of objects shows evidence for mixed chemistry. It is generally thought that the O-rich material represents dust formed during an earlier evolutionary phase of the star, possibly stored in a long-lived circumstellar disk.

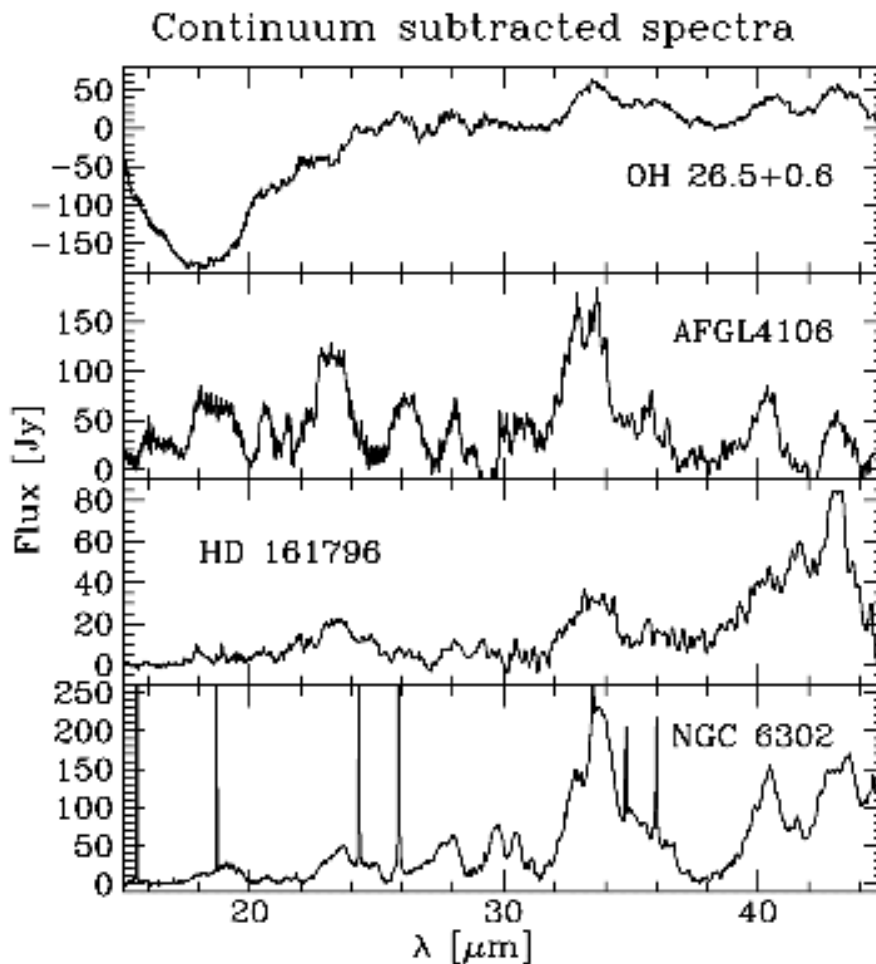


Figure 13. ISO-SWS spectra of a variety of objects illustrating the spectral diversity of stardust formed in the ejecta of AGB stars (Molster 2000).

After the AGB phase, as the central object evolves to the blue, the increased far-ultraviolet radiation and the strong outflows driven by its powerful winds process the envelope so that the spectral signatures of the dust and gas change. At this point, the infrared features of PAH molecules start to dominate the near- and mid-infrared spectra of C-rich objects. Many O-rich objects start to show evidence for crystalline silicates in their spectra ([Figure 13](#)).

Mid-infrared spectroscopy with NGST will revolutionize our understanding of the composition and evolution of the ejecta of AGB stars. Ground-based studies are limited to two atmospheric windows which miss much of the spectral richness. ISO studies of (post-)AGB objects have been limited to bright objects in the solar neighborhood, whereas SIRTf lacks spectral and spatial resolution. The mid-infrared instrument on NGST will be able to survey a large sample of late-type objects in galaxies from the local group out to the Virgo cluster. In this way a census of stardust can be built up and its dependence on the physical conditions (effective temperature, mass loss rate) including metallicity can be determined. These spectral characteristics can then also be compared to those of the interstellar medium in the host galaxy

to determine their interrelationship and investigate the dust mass balance of the galaxy.

High-mass stars evolve much more quickly and end their lives through a spectacular supernova explosion, expelling many heavy elements. NGST will have the sensitivity and spatial resolution to observe the in-situ formation of dust in knots with greatly different elemental abundances, such as the famous SN 1987A in the Large Magellanic Cloud.

II.9. Outer solar system: comets and KBOs

Comets are the most primitive objects in the solar system, formed in the outer regions of the solar nebula (see reviews by Irvine et al. 2000, Ehrenfreund & Charnley 2000). They therefore contain a precious record of the conditions that prevailed in the primitive solar nebula. These initial conditions are important constraints on models that describe the evolution of the solar nebula and the formation of the planets. So far, only limited information about the gas-phase and solid composition of comets has been obtained from mid-infrared observations, because of lack of instrumentation.

Infrared observations of comet Hale-Bopp with ISO provided CO₂ outgassing rates at different heliocentric distances, as well as data on the silicate emission (Crovisier et al. 1997). The dust shows (sometimes strong) evidence for substantial processing, and the mineral formation may point to complex radial mixing or heating processes in the solar nebula. New ground-based high spectral resolution near-infrared instruments are starting to provide information on minor organic species in comets, and it is becoming apparent that chemical differentiation exists amongst the comet population. For example, recent data from comet C/1999 S4 (LINEAR) show a greatly different composition compared with that of comets Halley, Hyakutake and Hale-Bopp (Mumma et al. 2001). Understanding this differentiation can put constraints on the place of cometary origin and on the chemical history of the organic material which formed them.

The NGST mid-infrared instrument will be able to observe comets when still far from perihelion when most volatiles are still in the cometary nucleus, and it will be able to monitor the development of the cometary tail as the temperature of the comet increases and dust and gas are released. It will have the sensitivity to obtain spectra of comets whose emission is a factor of 1000 times weaker than that of comet Hale-Bopp; several such comets will be visible to NGST each year.

The outer regions of the solar system are densely populated by a large number of bodies orbiting the Sun beyond Neptune. Up to 10⁵ objects are estimated to orbit in a distance of 30–50 AU from the Sun. Currently more than 400 Kuiper belt objects (KBO's) are detected and most of them have a diameter between 100 and 1200 km. These size estimates of KBO's are based on an assumed albedo of 0.04 (as for cometary nuclei) and those estimates may be considerably in error. The combination of optical data with simultaneous measurements of the thermal emission in the mid-infrared can determine both their size and albedo (Jewitt et al. 2001).

References

Aikawa, Y., van Zadelhoff, G.J., van Dishoeck, E.F., Herbst, E. 2001, A &A, submitted
André, P., Ward-Thompson, D., Barsony, M. 2000, in <i>Protostars & Planets IV</i> , eds. V.G. Mannings et al. (Univ. Arizona), p. 59
Artymowicz, P. 2001, in <i>Planetary systems in the universe</i> , IAU Symposium 202, eds. A. Penny et al. (San Francisco: ASP), in press
Aumann, H.H., Gillett, F.C., Beichman, C.A., et al. 1984, <i>ApJ</i> , 278, L23
Bacon, R., Copin, Y., Monnet, G., et al. 2001, <i>MNRAS</i> , 326, 23
Beckwith, S.V.W., Sargent, A.I. 1996, <i>Nature</i> , 383, 139
Bély, P., et al. 1998, NGST monograph no. 3 (Washington: GSFC)
Bernatowicz, T.J., Cowsik, R., Gibbons, P.C. et al. 1996, <i>ApJ</i> , 472, 760
Bertoldi, F., Timmermann, R., Rosenthal, D., Drapatz, S., Wright, C.M. 1999, A &A, 346, 267

Blain, A.W., Kneib, J.-P., Ivison, R.J., Smail, I. 1999, ApJ, 512, L87
Boogert, A.C.A. 1999, PhD Thesis, Univ. of Groningen
Bouwman, J., Meeus, G., de Koter, A., Hony, S., Dominik, C., Waters, L.B.F.M. 2001, A &A, in press
Burrows, A., Sharp, C.M. 1999, ApJ, 512, 843
Burrows, A., Marley, M., Hubbard, W.B., et al. 1997, ApJ, 491, 856
Burrows, C.J., Stapelfeldt, K.R., Watson, A.M. et al. 1996, ApJ, 473, 437
Cernicharo, J., Heras, A.M., Tielens, A.G.G.M., Pardo, J.R., Herpin, F., Guélin, M., Waters, L.B.F.M. 2001, ApJ, 546, L123
Chary, R., Elbaz, D. 2001, ApJ, 556, 562
Chiang, E.I., Joungh, M.K., Creech-Eakman, M.J., Qi, C., Kessler, J.E., Blake, G.A., van Dishoeck, E.F. 2001, ApJ, 547, 1077
Ciardi, B., Ferrara, A. 2001, MNRAS in press (astro-ph/0005461)
Crovisier, J., Leech, K., Bockelée-Morvan, D., et al. 1997, Science, 275, 1904
Draine, B.T., Bertoldi, F. 1999, in 'The Universe as seen by ISO', ESA SP-427, p. 553
Draine, B.T., Lee, H.M. 1984, ApJ, 285, 89
Dullemond, C., Dominik, C., Natta, A. 2001, ApJ, submitted
Dwek, E., Arrendt, R.G., Hauser, M.G. et al. 1998, ApJ, 508, 106
Ehrenfreund, P., Charnley, S. 2000, ARA &A, 38, 427
Ehrenfreund, P., Dartois, E., Demyk, K., d'Hendecourt, L. 1998, A &A, 339, L17
Elbaz, D., Cesarsky, C.J., Fadda, D., et al. 1999, A &A, 351, L37
Evans, N.J., Allen, L.E., Blake, G.A., et al. 2001, AAS meeting 198, 25.05 (http://sirtf.jpl.nasa.gov/SSC)
Genzel, R., Cesarsky, C. 2000, ARA &A, 38, 761
Genzel, R., Lutz, D., Sturm, E., et al. 1998, ApJ, 498, 579
Gerakines, P.A., Whittet, D.C.B., Ehrenfreund, P., et al. 1999, ApJ, 522, 357
Gibb, E., Whittet, D.C.B., Gerakines, P., et al. 2000, ApJ, 536, 347
Gispert, R., Lagache, G., Puget, J.L. 2000, A &A, 360, 1
Greaves, J.S., Holland, W.S., Moriarty-Schieven, G., et al. 1998, ApJ, 506, L133
Habing, H.J., Dominik, C., Jourdain de Muizon, M., et al. 1999, Nature, 401, 456
Haiman, Z., Loeb, A. 1998, ApJ, 503, 505
Haisch, K.E., Lada, E.A., Lada, C.J. 2001, ApJ, 553, L153
Hanson, M.M., Howarth, I.D., Conti, P.S. 1997, ApJ, 489, 698
Holland, W.S., Greaves, J.S., Zuckerman, B., et al. 1998, Nature, 392, 788
Irvine, W.M., Schloerb, F.P., Crovisier, J., Fegley, B., Mumma, M.J. 2000, in Protostars & Planets IV, eds. V.G. Mannings et al. (Univ. Arizona), p. 1159
Jewitt, D., Aussel, H., Evans, A. 2001, Nature, 411, 446

Kirkpatrick, J.D. 2001, in 'Galactic structure, stars and the interstellar medium', eds. C.E. Woodward et al. ASP Vol. 231 (San Francisco: ASP), p. 17
Koerner, D.W., Ressler, M.E., Werner, M.W., Backman, D.E. 1998, ApJ, 505, 358
Kramer, C., Alves, J., Lada, C.J., et al. 1999, A &A, 342, 257
Lada, C.J., Alves, J., Lada, E.A. 1999, ApJ, 512, L250
Langer, W.D., van Dishoeck, E.F., Blake, G.A., Bergin, E., Tielens, A.G.G.M., Velusamy, T., Whittet, D.C.B. 2000, Protostars & Planets IV, eds. V. Mannings, A. Boss, S. Russell (Tucson: Univ. of Arizona), p. 27
Le Floch, E., Mirabel, I.F., Laurent, O. et al. 2001, A &A, in press (astro-ph/0101038)
Lenorzer, A., Bik, A., Kaper, L., et al. 2001, A &A, to be submitted
Lutz, D., Spoon, H.W.W., Rigopoulou, D., Moorwood, A.F.M., Genzel, R. 1998, ApJ, 505, L103
Malfait, K., Waelkens, C., Waters, L.B.F.M., Vandebussche, B., Huygen, E., de Graauw, Th., 1998, A &A, 332, L25
Marcy, G.W., Butler, R.P. 1996, ApJ, 464, L147
Mayor, M., Queloz, D. 1995, Nature, 378, 355
McCaughrean, M.J., O'Dell, C.R. 1996, AJ, 111, 1977
Meeus, G., Waters, L.B.F.M., Bouwman, J., van den Ancker, M.E., Waelkens, C., Malfait, K. 2001, A &A, 365, 476
Mirabel, I.F., Vigroux, L., Charmandaris, V., Sauvage, M., Gallais, P., Tran, D., Cesarsky, C., Madden, S.C., Duc, P.A. 1998, A &A, 333, L1
Mirabel, I.F., Laurent, O., Sanders, D.B. et al. 1999, A &A, 341, 667
Molster, F.J., Yamamura, I., Waters, L.B.F.M. et al. 1999, Nature 401, 563
Molster, F.J. 2000, PhD Thesis, University of Amsterdam
Morris, P.W., Waters, L.B.F.M., Barlow, M.J., Lim, T., de Koter, A., Voors, R.H.M., Cox, P., de Graauw, Th., Henning, Th., Hony, S., Lamers, H.J.G.L.M., Mutschke, H., Trams, N.R. 1999, Nature, 402, 502
Mouillet, D., Larwood, J.D., Papaloizou, J.C.B., Lagrange, A.M. 1997, MNRAS, 292, 896.
Mumma, M.J., Dello Russo, N., DiSanti, M.A., et al. 2001, Science, 292, 1334
Oliver, S., Mann, R.G., Carballo, R., Franceschini, A., Rowan-Robinson, M., Kontizas, M., Dapergolas, A., Kontizas, E., Verma, A., Elbaz, D., Granato, G.-L., Silva, L., Rigopoulou, D., Gonzalez-Serrano, J.I., Serjeant, S., Efstathiou, A., Van der Werf, P.P., MNRAS, submitted
Padgett, D.L., Brandner, W., Stapelfeldt, K.R., Strom, S.E., Terebey, S., Koerner, D. 1999, AJ, 117, 1490
Papovich, C.J., Dickinson, M., Ferguson, H.C. 2001, ApJ, in press (astro-ph/0105087)
Schutte, W.A., Greenberg, J.M. 1997, A &A, 317, L43
Schutte, W.A., et al. 2001, A &A, submitted
Serabyn, E. et al. 1999, A mid-infrared camera for NGST, (http://www701.gsfc.nasa.gov/isim/science)

Stahler, S., Palla, F., Ho, P.T.P. 2000, in <i>Protostars & Planets IV</i> , eds. V. Mannings, A. Boss, S. Russell (Tucson: Univ. of Arizona), p. 327
Stockman, P., ed., 1997, 'NGST: Visiting a time when galaxies were young' (Associated Univ.)
Thi, W.F., van Dishoeck, E.F., Blake, G.A., van Zadelhoff, G.J., Hogerheijde, M.R. 1999, <i>ApJ</i> , 521, L63
Thi, W.F., Blake, G.A., van Dishoeck, E.F., et al. 2001a, <i>Nature</i> , 409, 60
Thi, W.F., van Dishoeck, E.F., Blake, G.A. et al. 2001b, <i>ApJ</i> , in press (astro-ph/0107006)
Tielens, A.G.G.M. 2001, in 'Galactic structure, stars and the interstellar medium', ed. C.E. Woodward et al. (San Francisco: ASP), p. 92
Tielens, A.G.G.M., van Kerckhoven, C., Peeters, E., Hony, S. 2000, in 'Astrochemistry: from molecular clouds to planetary systems', IAU Symposium 197, eds. Y.C. Minh & E.F. van Dishoeck (San Francisco: ASP), p. 349
van den Ancker, M.E., Wesselius, P.R., Tielens, A.G.G.M. 2000, <i>A & A</i> , 355, 194
van Dishoeck, E.F. 2000, in 'NGST science and technology exhibition', eds. E. Smith and K. Long, ASP Vol. 207 (San Francisco: ASP), p. 85
van Dishoeck, E.F., Blake, G.A. 1998, <i>ARA & A</i> , 36, 317
van Dishoeck, E.F., Wright, C.M., Cernicharo, J., González-Alfonso, E., Helmich, F.P., de Graauw, Th., Vandenbussche, B. 1998, <i>ApJ</i> , 502, L173
van Zadelhoff, G.J., Thi, W.F., van Dishoeck, E.F., Blake, G.A. 2001, <i>A & A</i> , in press
von Helden, G., Tielens, A.G.G.M., van Heijnsbergen, D., Duncan, M.A., Hony, S., Waters, L.B.F.M., Meijer, G. 2000, <i>Science</i> , 288, 313
Waelkens, C., Waters, L.B.F.M., de Graauw, Th., et al. 1996, <i>A & A</i> , 315, L245
Waters, L.B.F.M., Waelkens, C. 1998, <i>ARA & A</i> , 36, 233
Waters, L.B.F.M., Molster, F.J., Waelkens, C. 1999, in 'Solid interstellar matter: the ISO revolution', eds L. d'Hendecourt et al. (EDP, Springer), p. 219
Waters, L.B.F.M., Molster, F.J., de Jong, T., et al. 1996, <i>A & A</i> , 315, L361
Wright, C.M. 2000, in 'Astrochemistry: from Molecular Clouds to Planetary Systems', eds. Y.C. Minh & E.F. van Dishoeck, IAU Symposium 197 (ASP), p. 177
Wright, C.M., van Dishoeck, E.F., Cox, P., Sidher, S.D., Kessler, M.F. 1999, <i>ApJ</i> , 515, L29
Wright, G., Posselt, W. et al. 1999, MIRCAM and MIRIFS, (http://www701.gsfc.nasa.gov/isim/science)

APPENDIX F. Abbreviations

AGB	Asymptotic Giant Branch
AGN	Active Galactic Nucleus
AIT	Assembly, Integration and Testing
ALMA	Atacama Large Millimeter Array
AMOLF	Institute for Atomic and Molecular Physics
ASTRON	Stichting ASTRonomisch Onderzoek in Nederland
ASWG	Ad-Hoc Science Working Group of NGST
ATC	Astronomy Technology Centre in Edinburgh, UK
AURA	Association of Universities for Research in Astronomy
AWG	Astronomy Working Group of ESA
AU	Astronomical Unit
BD	Brown Dwarf
BRDF	Bidirectional Reflection Distribution Function
CAD/CAM	Computer Aided Design / Computer Aided Manufacturing
CNC	Computer Numerically Controlled
CSA	Canadian Space Agency
DARWIN	ESA's infrared space interferometry mission (also known as IRSI)
DENIS	Deep Near Infrared Southern Sky Survey
DRM	Design Reference Mission of NGST
ECF	European Coordinating Facility
EGP	Extrasolar Giant Planet
EOS	Earth Observing System
ESA	European Space Agency
ESO	European Southern Observatory
ESTEC	European Space Research and Technology Centre in Noordwijk
FIRST	Far-Infrared and Submillimeter Space Telescope (renamed to Herschel)
FOM	Fundamenteel Onderzoek der Materie
GSFC	Goddard Space Flight Center
GOME	Global Ozone Monitoring Experiment
HDF	Hubble Deep Field
HIFI	Heterodyne Instrument for the Far-Infrared on Herschel

HST	Hubble Space Telescope
HSO	Herschel Space Observatory (formerly known as FIRST)
IDP	Interplanetary Dust Particle
IFU	Integral Field Unit
IMF	Initial Mass Function
IRAC	InfraRed Array Camera on SIRTf
IRAS	InfraRed Astronomical Satellite
IRS	InfraRed Spectrograph on SIRTf
IRSI	InfraRed Space Interferometry mission of ESA (also known as DARWIN)
ISO	Infrared Space Observatory
ISOCAM	CAMera on ISO
ISOSWS	Short Wavelength Spectrometer on ISO
ISWG	Interim Science Working Group of NGST
JCMT	James Clerk Maxwell Telescope
KBO	Kuiper Belt Object
KMWE	Klein Mechanische Werkplaats Eindhoven
LMC	Large Magellanic Cloud
LRS	Low Resolution Spectrometer (IRAS)
LWS	Long Wavelength Spectrometer (ISO)
2MASS	2 Micron All Sky Survey
MICHELLE	MIdinfrared eCHELLE spectrometer on UKIRT/Gemini
MIDI	MID-infrared Interferometric instrument for the VLTI
MIPS	Multiband Imaging Photometer on SIRTf
MIRPPG	Mid-InfraRed Partnership Planning Group of NGST
MISC	Mid-Infrared Steering Committee of NGST
METOP	Meteorological Operational polar satellites of EUMETSAT
NASA	National Aeronautics and Space Administration of the USA
NGST	Next Generation Space Telescope
NICMOS	Near Infrared Camera and Multi-Object Spectrometer on HST
NLR	Nationaal Lucht en Ruimtevaartlaboratorium
NOVA	Nederlandse Onderzoekschool voor Astronomie
OGSE	Optical Ground Support Equipment
OMI	Ozon Monitoring Instrument

PA	Product Assurance
PAH	Polycyclic Aromatic Hydrocarbon
PDR	Photo-Dissociation Region or Photon-Dominated Region
PI	Principal Investigator
QA	Quality Assurance
RAL	Rutherford Appleton Laboratory
RuG	RijksUniversiteit Groningen
SAP	Service d'Astrophysique in Saclay
SAURON	Spectrographic Areal Unit for Research on Optical Nebulae
SCIAMACHY	SCanning Imaging Absorption SpectroMeter for Atmospheric CHartographY
SCUBA	Submillimeter Common User Bolometer Array (JCMT)
SED	Spectral Energy Distribution
SIRTF	Space InfraRed Telescope Facility
SKA	Square Kilometer Array
SLOAN	Sloan Digital Sky Survey
SOFIA	Stratospheric Observatory For Infrared Astronomy
SRON	Space Research Organization Netherlands
TNO	Toegepast Natuurwetenschappelijk Onderzoek
TPD	Technisch Fysische Dienst
TPF	Terrestrial Planet Finder
UKIRT	United Kingdom InfraRed Telescope
UL	Universiteit Leiden
ULIRG	UltraLuminous InfraRed Galaxy
UvA	Universiteit van Amsterdam
VISIR	VLT Mid Infrared Spectrometer/Imager
VLT	Very Large Telescope of ESO
VLTI	Very Large Telescope Interferometer of ESO
WBS	Work Breakdown Structure
WFPC	Wide Field Planetary Camera on HST
WHT	William Herschel Telescope on La Palma
WSRT	Westerbork Synthese Radio Telescoop

Email: ASTRON project manager: [Lars Venema](#)

This file: [Jaap Tinbergen](#)



Dwingeloo, Netherlands.

[ASTRON](#) is the official name of the Netherlands Foundation for Research in Astronomy NFRA).